CHAPTER 4

ANALYSIS OF DATA AND DISCUSSION OF RESULTS

4.1 Characterization of Materials

4.1.1 DSC Analysis of Unmodified and Modified Epoxy

Curing is an important aspect that needs to be considered when dealing with polymeric materials. A polymer needs to be fully cured to optimize its mechanical properties [119]. To measure how far the curing reaction has progressed is by determining the degree of cure, *p*.

During the curing reactions and in order for a polymer to form networks, the polymer undergoes two main transitions: gelation and vitrification. When gelation occurs, the system has actually transformed from a liquid into a covalently crosslinked gel, while vitrification is a transformation of the system from a liquid/gel into a glassy state. The transitions involved in the formation of a polymer network are shown in Figure 4.1 [120].

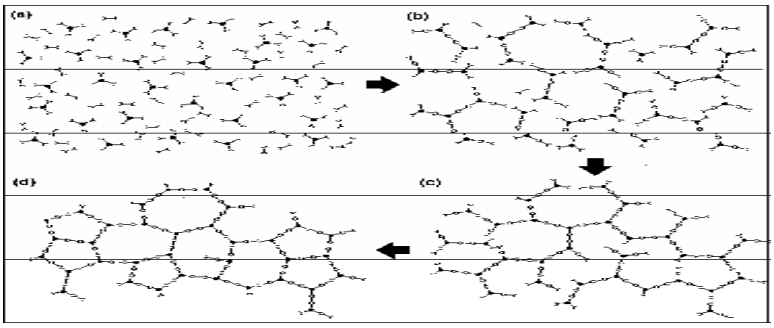

Fig. 4.1 Transitions involved in the formation of a polymer network [120]

The vitrification process occurs due to reduction of the system's mobility through the formation of covalent bonds, and this is associated with the glass transition temperature, T_g. Glass transition, is the temperature at which amorphous polymers undergo a second order transition from being glassy (hard and brittle) to being rubbery (elastomeric and flexible).

Figure 4.2 indicates the DSC thermograms for unmodified system of epoxy (Blank 1 sample), which had been cured at room temperature. Meanwhile, Figure 4.3 indicates the DSC thermograms of the modified epoxy coating samples in the first heating cycle. The different curves in the figure correspond to the glass transitions obtained for samples A, B and C containing various epoxy-PANI formulations and had been cured at room temperature (RT). The values of Tg derived from these thermograms are tabulated in Table 4.1.

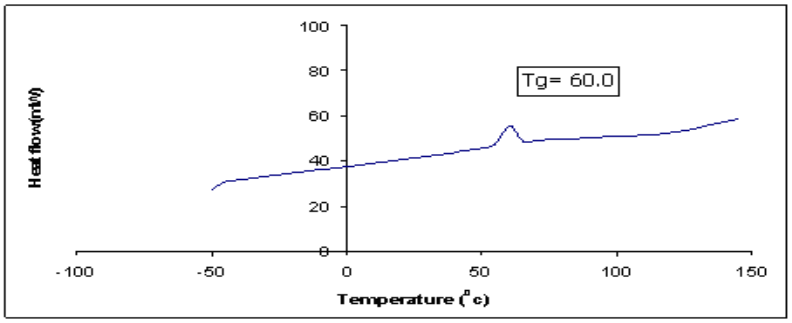

Fig. 4.2 DSC thermogram for Blank 1 sample

Table 4.1 Glass transition values for samples cured at room temperature

SAMPLES (cured at RT)	**GLASS TRANSITION, Tg (° C)**
BLANK 1 (PANI 0%)	60± 1
A (PANI 0.5%)	68± 1
B (PANI 1.0%)	64± 1
C (PANI 1.5 %)	63± 1

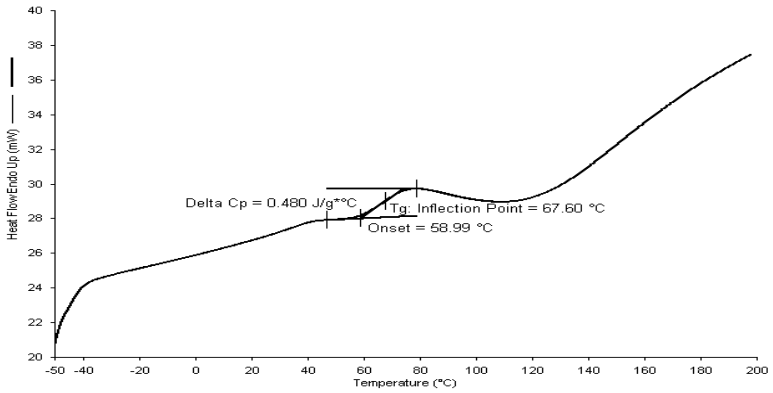

(a) Sample A (indicates 0.5% of PANI)

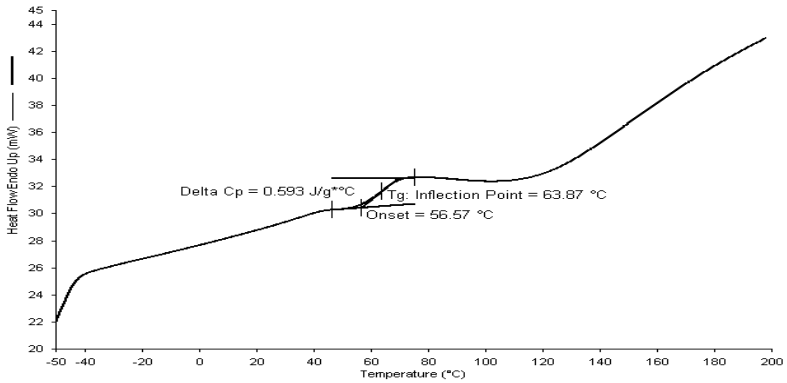

(b) Sample B (indicates 1.0% PANI)

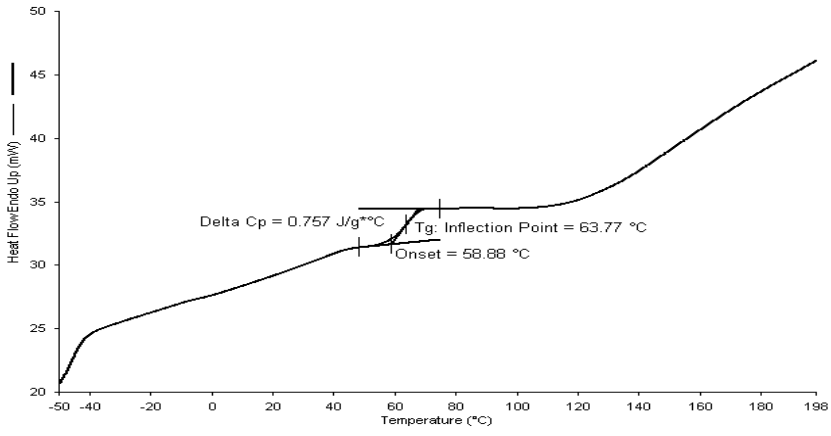

(c) Sample C (indicates 1.5% PANI)

Fig. 4.3 DSC thermograms for modified samples cured at room temperature

The glass transition value of the Blank 1 sample is 60± 1, while the Tg values for sample A, B and C are 68± 1, 64± 1 and 63± 1 respectively. Sample with 0.5 % of PANI content exhibits the highest value of Tg, and the Blank sample exhibits the lowest value of Tg. The glass transition values decrease in the order: A > B > C> Blank 1.

Water absorption is a common phenomenon relating to epoxy and other polymeric materials. Epoxy has a very high tendency to absorb water. This is undesirable particularly when the polymeric material is used as coatings because when water is absorbed, it will contribute to corrosion phenomena. In an epoxy system, water may be absorbed when the epoxy is not fully reacted. When the samples were cured at room temperature, the epoxy has not been fully reacted. Referring to Figure 4.4, the amount of unreacted epoxy can be determined by calculating the degree of cure using Equation 4.1 [120].

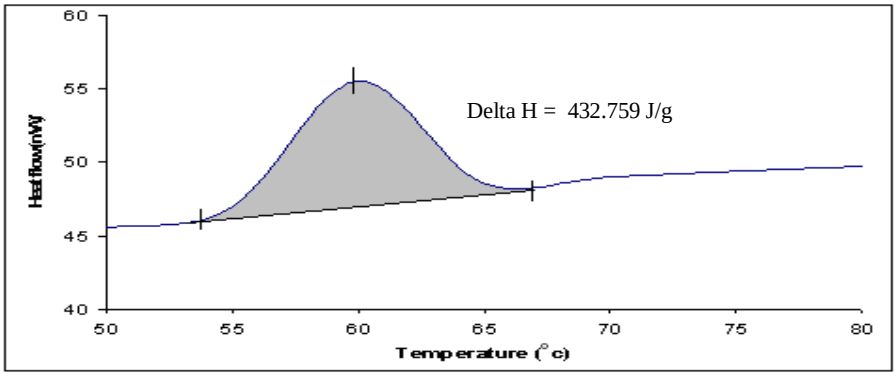

Fig. 4.4 DSC thermograms of unreacted epoxy/m-XDA

$$\text{Degree of cure, } p = 1 - \frac{\Delta H_t}{\Delta H_{unreacted}} \qquad \text{Eq. 4.1}$$

To obtain the value of $\Delta H_{unreacted}$, epoxy and m-XDA were mixed in the aluminum cup and DSC analysis was performed immediately after the mixing. The value of $\Delta H_{unreacted}$ obtained was approximately 432.759 J/g. The values of ΔH_t for all samples cured at room temperature are shown in Figure 4.5 . Meanwhile the values of degree of cure are as shown in Table 4.2 and these values indicating that the epoxy was not

fully cured. When an epoxy is not 100% cured, it is expected that more water will be absorbed by the epoxy and this will give a significant effect on corrosion.

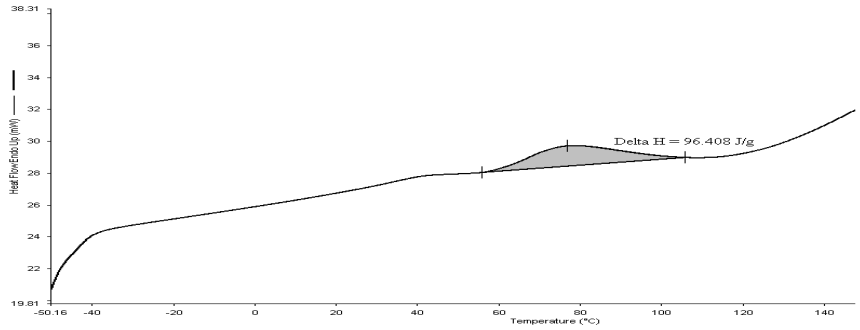

(a) Sample A (indicates 0.5% PANI)

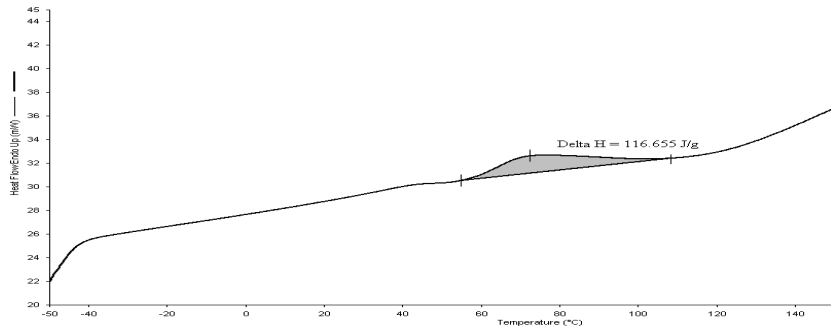

(b) Sample B (indicates 1.0% PANI)

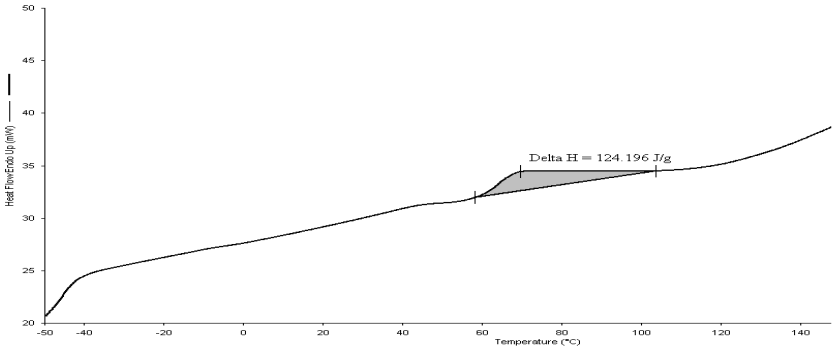

(c) Sample C (indicates 1.5% PANI)

Fig. 4.5 DSC thermograms indicating the ΔH_t values of modified samples cured at room temperature (RT)

Table 4.2 The values of degree of cure, p for all modified samples cured at RT

Samples	**ΔH_t (J/g)**	**Degree of cure, p**	**Degree of cure by percentage (%)**
Sample A	96.408	0.78	78
Sample B	116.655	0.73	73
Sample C	124.196	0.71	71

From Table 4.2, the degree of cure for sample A, sample B and sample B were 0.78, 0.73 and 0.71 respectively. These values indicate that all samples were not fully crosslinked as a fully crosslinked sample represented by p=1 or p=100%. It can also be seen from the table that sample C exhibits the lowest value of degree of cure compared to sample A and sample B which indicates that sample C exhibit the lowest crosslinking where the sample only 71% cured. The degree of cure indicates how far the reaction has progressed and crosslinked. Based on the values of degree of cure of all samples, it is expected that sample A will absorb the lowest amount of water while sample C will absorb the highest amount of water.

On the other hand, the DSC curves for samples containing various epoxy-PANI formulations namely D, E and F cured at 120° C are shown in Figure 4.6 and the thermogram for a Blank sample cured at the same temperature is shown in Figure 4.7. The glass transition values for these samples are tabulated in Table 4.3. The Tg values of Blank 2, sample D, E and F are 105± 1, 114± 1, 111± 1 and 109± 1 respectively. The Tg values decrease in the following manner: D > E > F > Blank 2.

As can be observed from Figures 4.6, the DSC curves of samples D, E and F reached a plateau when reaching 120° C, which indicate that the epoxy samples were fully cured at 120° C. A maximum glass transition temperature, Tg was obtained for all three samples. This will produce epoxies with optimized mechanical properties. Thus minimum water absorption by the epoxies is expected and therefore, corrosion could be reduced.

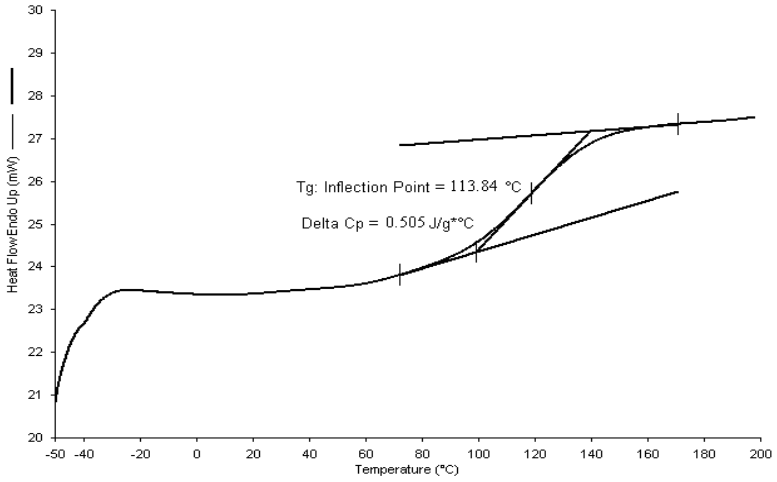

(a) Sample D (% PANI)

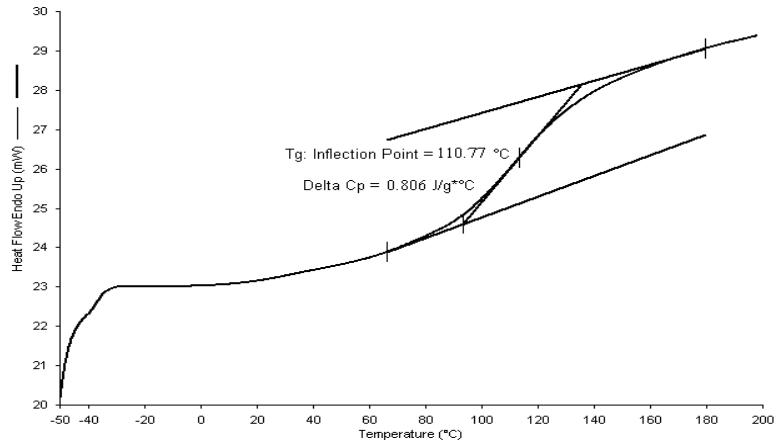

(b) Sample E (% PANI)

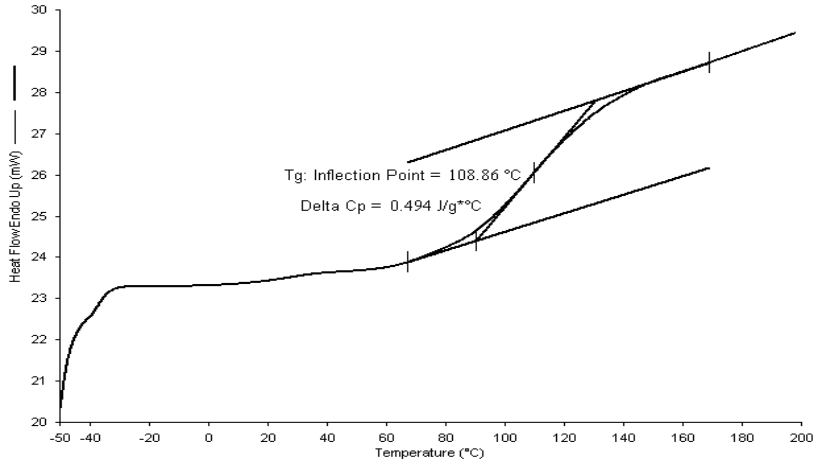

(c) Sample F (% PANI)

Fig. 4.6 DSC thermograms for modified samples cured at 120° C

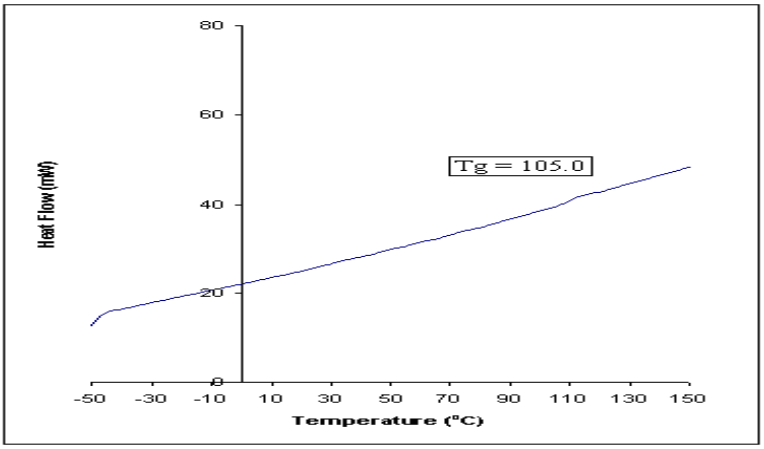

Fig. 4.7 DSC thermogram of Blank 2 sample

Table 4.3 Glass transition values for samples cured at 120° C

SAMPLES (cured at 120° C)	**GLASS TRANSITION, Tg (°C)**
BLANK 2 (PANI 0%)	105± 1
D (PANI 0.5%)	114± 1
E (PANI 1.0%)	111± 1
F (PANI 1.5 %)	109± 1

In general, samples cured at 120° C have higher Tg values compared to samples cured at room temperature (RT). It is also observed that sample with 0.5% PANI content exhibits the highest Tg values and the Blank sample exhibits the lowest Tg values for both conditions (120° C and RT). However, sample D has the highest Tg value (114± 1) among all samples regardless of the curing conditions. The effect of adding PANI into the epoxy system revealed that Tg of the modified system is decreased as the amount of PANI is increased, where $Tg_{PANI\ 1.5\%} < Tg_{PANI\ 1.0\%} < Tg_{PANI\ 0.5\%}$. While the epoxy without PANI (Blank sample) exhibits lowest Tg values for each curing condition. The overall comparison is shown in Figure 4.8.

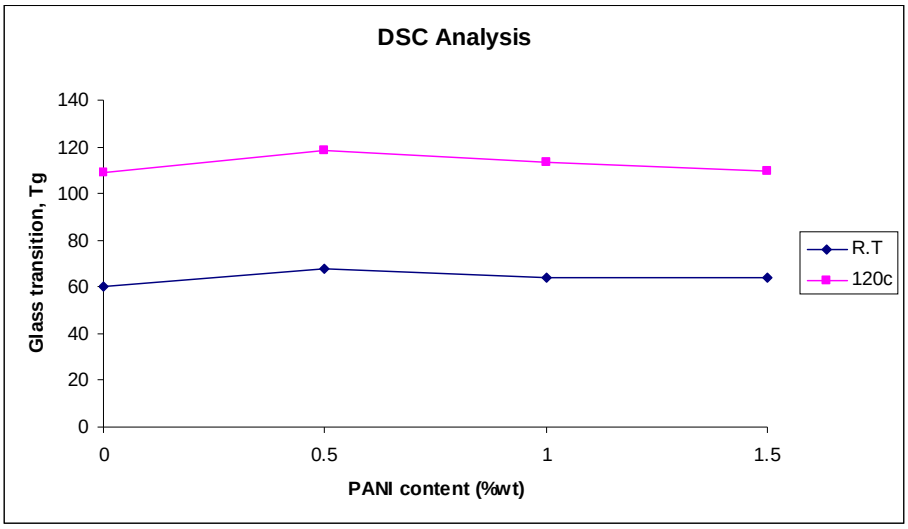

Fig. 4.8 Comparison of Tg values between RT and 120°C

Based on the glass transition values obtained, it is most probable that sample D, which has the highest Tg value, will exhibit the best mechanical properties; thus providing the best corrosion protection compared to other samples. This prediction will be supported by the results of water absorption and pull-off test results which will be discussed in section 4.4 and 4.5.

4.1.2 TGA Analysis of Unmodified and Modified PANI

The TGA analysis was done to determine the thermal stability of all unmodified and modified epoxy samples. Thermal stability is a description of the chemical stability of polymer at high temperature, since chemical processes that take place at elevated temperatures results in thermal degradation or cross-linking of high polymers [53]. Thermal analysis is very important since it reveals the limiting point of temperature that a material can withstand.

The results of thermal analysis for unmodified epoxy (Blank samples) for both curing conditions are shown in Figure 4.9, while the thermal analysis for modified epoxy samples cured at RT and 120^{o} C are shown in Figures 4.10 and 4.11, respectively. The TG curves are between 42° C to 600° C. Based on the

thermograms, generally, all samples remained stable until 300° C. For unmodified epoxy (Fig. 4.9), the onset of degradation for Blank 1 sample starts to occur at about 309 ± 1° C, while the degradation for Blank 2 sample starts to occur at 311 ± 1° C. This shows that the unmodified epoxy that has been fully cured at 120° C has better thermal stability than the unmodified epoxy cured at RT. Thus the fully cured epoxy is expected to have better thermal properties than the unmodified epoxy that had not fully reacted (cured at RT).

The addition of Polyaniline in the epoxy system, within the range of concentration in this study, has no significant effect on the thermal behavior; where no changes in the thermal behavior was observed even when the highest concentration was used (1.5% PANI). However, the onset of degradation for all samples was different from each other. For modified samples cured at RT (Figure 4.10), the onset of degradation for samples A, B and C started at 315 ± 1° C, 314 ± 1° C and 312 ± 1° C, respectively. This indicates that thermal stability of the samples decreases in the order A > B > C.

Meanwhile, for modified samples cured at 120° C (Figure 4.11), the onset of degradation for samples D, E and F started at 324 ± 1° C, 320 ± 1° C and 317 ± 1° C. Similar to samples cured at RT, the samples with lower PANI loading are more thermally stable (sample with 0.5% PANI has the highest thermal stability). Thermal stability of the samples decreases in the order D> E> F. The overall results for unmodified and modified epoxies are shown in Table 4.4.

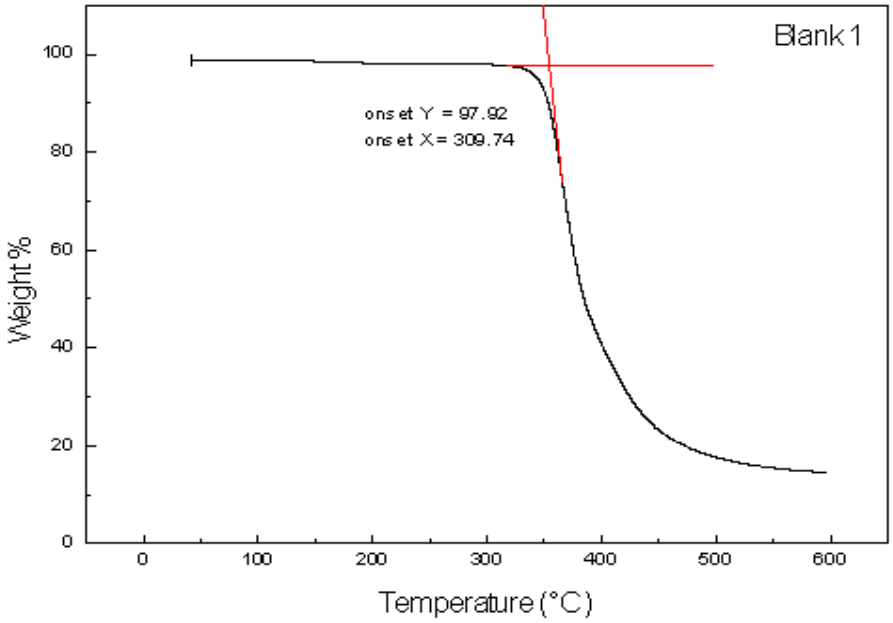

(a)

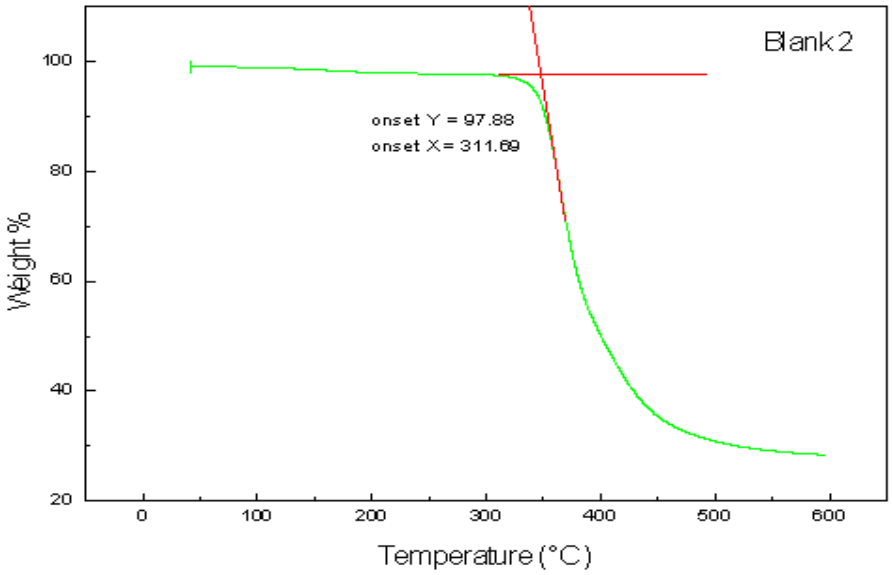

(b)

Fig.4.9 TGA thermograms of unmodified epoxy cured at (a) RT and (b) 120° C

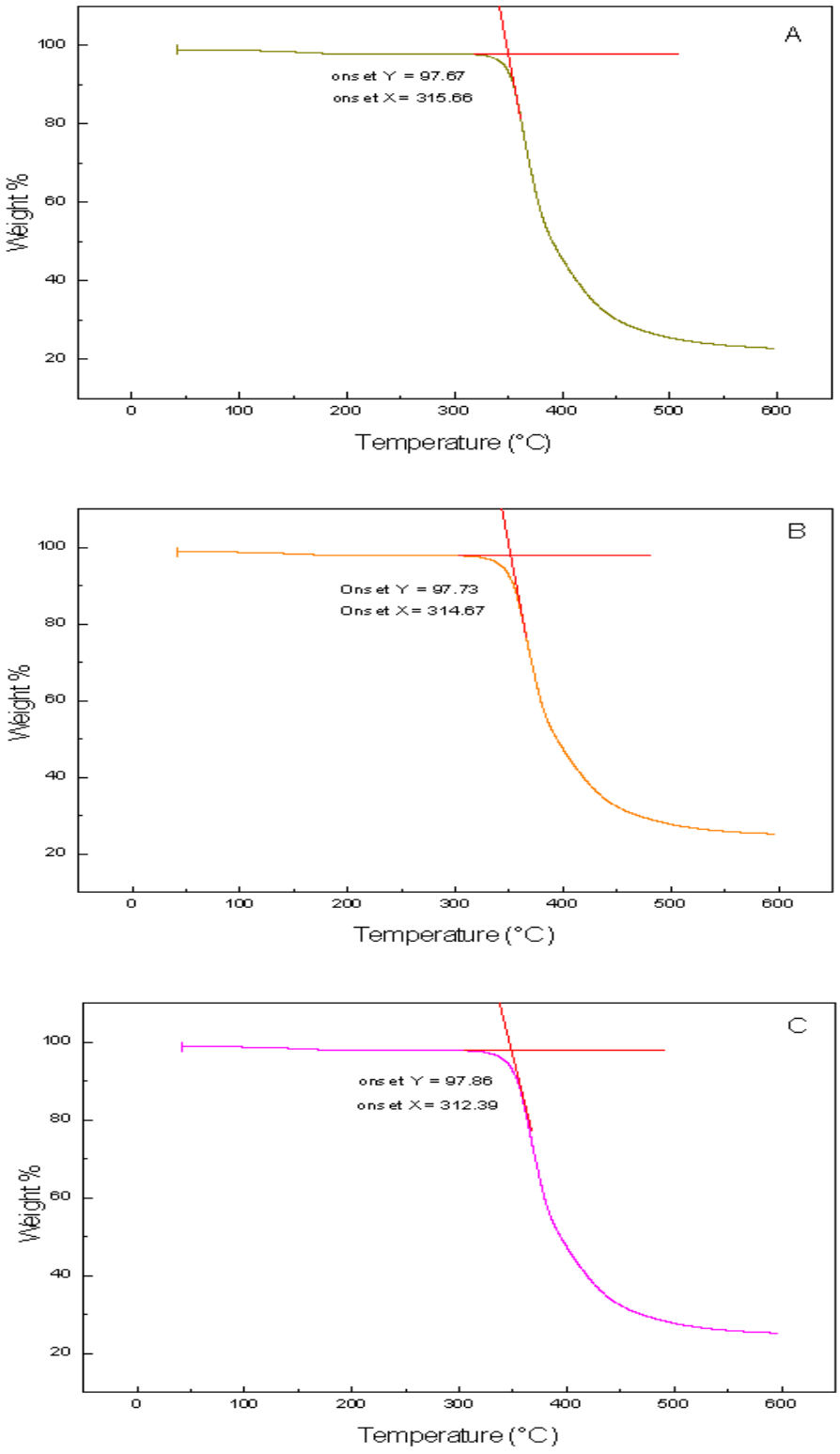

Fig. 4.10 TGA thermograms of modified epoxy cured at RT

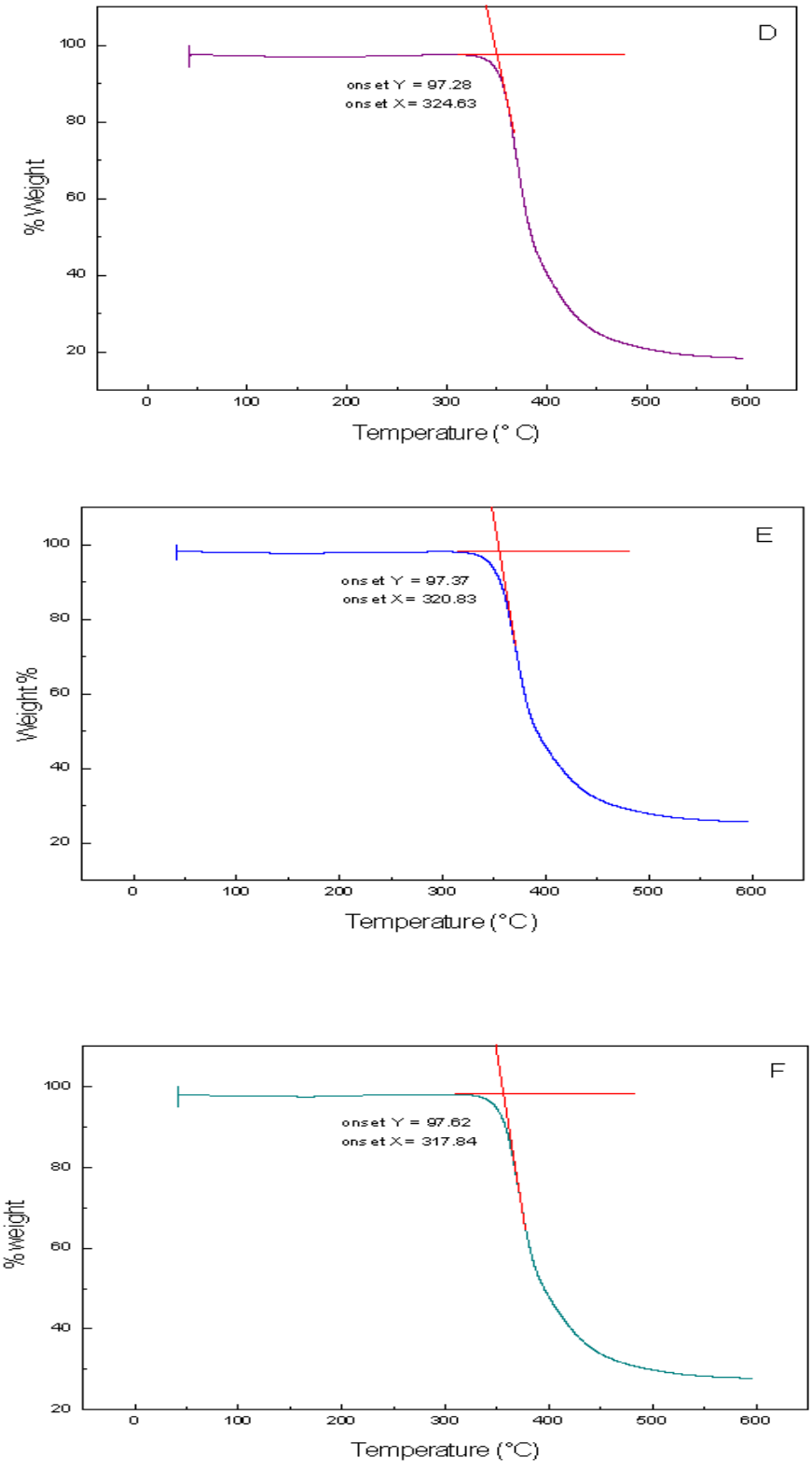

Fig. 4.11 TGA thermograms of modified epoxy cured at 120°C

Table 4.4 Thermal properties by TGA analysis

SAMPLES	T_{onset} degradation (° C)
BLANK 1	309 ± 1
BLANK 2	311 ± 1
A (PANI 0.5%) -RT	315 ± 1
B (PANI 1.0%) -RT	314 ± 1
C (PANI 1.5%) - RT	312 ± 1
D (PANI 0.5%) – 120 °C	324 ± 1
E (PANI 1.0%) – 120 °C	320 ± 1
F (PANI 1.5%) – 120 °C	317 ± 1

When comparing all the results, obviously samples cured at 120^{o} C have higher thermal stability than samples cured at room temperature. One of the reasons for this is because of the crosslink density. The glass transition temperature, Tg for fully cured samples (samples cured at 120^{o} C) are higher than samples that are not fully cured (samples cured at RT) as shown in Tables 4.1 and 4.3. These findings are supported by [88], in which he claimed that the network structure and crosslink density will determine the thermal stability of epoxy resins. The higher the crosslink density, the more thermal stability will be achieved as there is less free volume in the epoxy.

On the other hand, the addition of Polyaniline has also caused the thermal stability to increase. However, with the increase of PANI from 0.5% to 1.0% and 1.5%, the thermal stability dropped, but still higher than the samples without PANI (Blank/ unmodified samples). This proves that the addition of PANI could increase the thermal stability of the epoxy systems, thus improving the thermal properties of the materials. This could be explained by the phase-plasticizer effect by PANI in which the presence of PANI does not cause phase-plasticizer effect to the chain. PANI which was mixed at nano level improves the Tg. It restricts the chain movements, therefore increasing the Tg. In addition, the lower thermal stability of samples cured at RT and samples with high PANI content could be related to an increase in free volume of the samples. This seems to be in agreement with the greater amount of

water being absorbed by samples containing higher amount of PANI; this will be explained in detail in section 4.4.

4.1.3 FTIR Analysis of Unmodified and Modified Epoxy

The functional groups contained in the epoxy systems which absorb in the mid infrared region that lies between 4000 cm^{-1} to 400 cm^{-1} were identified by FTIR analysis. FTIR absorption spectra of pure PANI, unmodified epoxy (without PANI) and modified epoxy (with PANI) are shown in Figure 4.12. Generally, the spectra of the modified epoxy system are almost identical to those of the original (unmodified) epoxy system. This indicates that there were no alteration in the epoxy-based resin by the addition of small concentrations of Polyaniline.

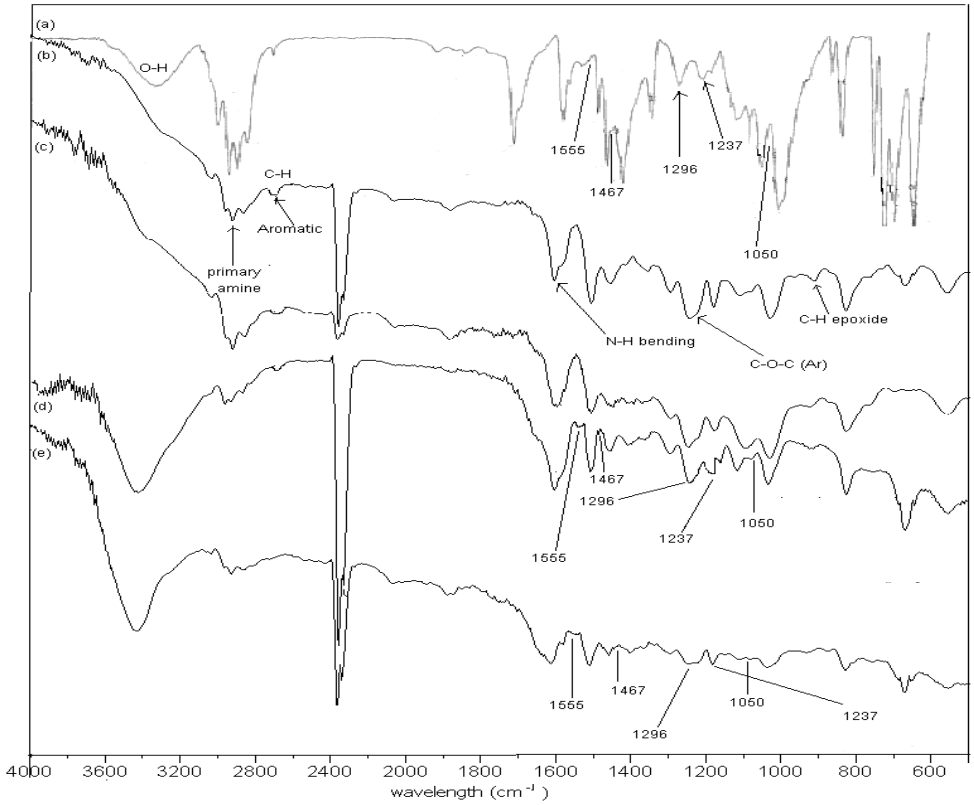

Fig.4.12 IR absorption spectra of (a) pure PANI (b) unmodified epoxy cured at RT (c)unmodified epoxy cured at 120° C (d) modified epoxy (1.5% PANI) cured at RT (e) modified epoxy cured at 120° C (1.5% PANI)

The IR spectra for pure PANI shows the presence of peaks around 1555, 1467, 1296, and 1237 cm^{-1} which confirmed the structure of PANI since these peaks are the important characteristics peaks of the emeraldine salt structure. The IR absorption bands at 1555 and 1467 cm^{-1} are the characteristic bands due to C=N and C=C of quinonoid and benzenoid rings respectively. The absorption band at 1237 and 1296 cm^{-1} are due to C-N stretching of secondary amine in the polymer chain. The peaks present at those particular bands are characteristics of the conducting polaron structure C-N+ of doped PANI associated with oxidation or protonation states of PANI [8], [14], [105], [109] and [121]. Since the Polyaniline used in the epoxy system was derived from the doping of aniline with sulfonic acid group, the peak that appears at 1050 cm^{-1} is therefore due to the presence of the sulfonic group [8].

The unmodified epoxy system consists of Epikote 828 and its curing agent, m-XDA, while the modified epoxy system consists of both Epikote 828/m-XDA with the addition of PANI. For unmodified epoxy (b) and (c), the presence of strong bands in the 1247 cm^{-1} region was identified as ArC-O-C-alkyl (ether group) of the thermo-stable polymer bisphenol A, which is typically found in epoxy resins. Meanwhile, the two spikes at around 3500-3200 cm^{-1} indicated the characteristic of primary amine, which confirmed the structure of *m*-XDA [14] and [46].

For modified epoxy (d) and (e), the IR spectra obtained were almost similar to the unmodified epoxy. However, the peaks that confirm the structure of PANI as observed in spectra (a) (pure PANI) were observed to appear in these modified epoxy spectra. This proved the existence of PANI in the modified samples. The complete interpretation of the absorption bands of both epoxy systems are presented in Tables 4.5 and 4.6.

In addition, the modified epoxy system has three different formulations where the amount of PANI was varied from 0.5-1.5%. It was observed that the IR spectra for all the other modified epoxy samples have similar absorption bands the (d) and (e) IR spectra regardless of the percentage of PANI in the epoxy.

Table 4.5 Interpretation of absorption bands for unmodified epoxy

Wave number region (cm^{-1})	Functional group
3000-3700	O-H
3200-3500	N-H stretching, primary amine
3050	C-H aromatic
2927	CH_2 methyl C-H asymmetric
2872	CH_3 methyl C-H sym
1607	C=C aromatic band
1505	C=C aromatic band
1296	Ar-C-O-C-R (ether)
1182	C-H aromatic
1031	C-H aromatic
917	C-H terminal epoxide
823	C-H aromatic

Table 4.6 Interpretation of absorption bands for modified epoxy

Wave number region (cm^{-1})	Functional group
3000-3700	O-H
3200-3500	N-H stretching, primary amine
3056	CH_2 epoxy
2927	CH_2 methyl C-H asymmetric
2872	CH_3 methyl C-H sym
1505, 1607	C=C aromatic band
1467	C=C benzenoid ring
1296	C-N stretching, secondary amine
1237	C-N structure in bipolaron structure
1110	vibration of protonated doped PANI
1050	SO_3^- group
917	C-H terminal epoxide
800	1,4-para substituted benzene ring

4.2 Surface Profile Test

The purpose of performing this test was to measure the surface roughness (R_a) and surface roughness depth (R_z) of the samples (mild steel). These values are the indicator whether the samples are ready to be coated or not. The measurement was done based on an average of three samples. The test results are shown in Figure 4.13 and the average of the measurements is tabulated in Table 4.7.

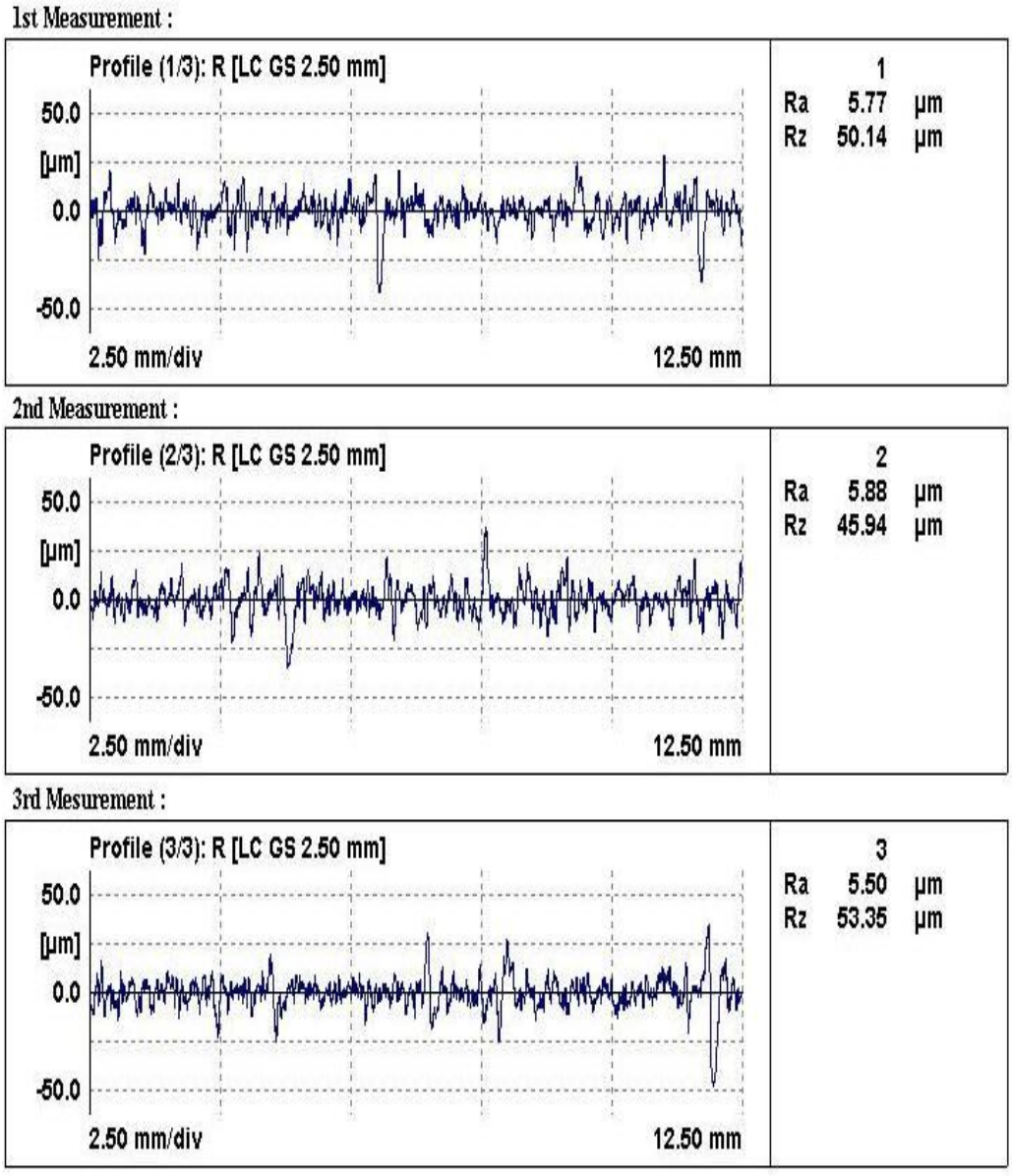

Fig. 4.13 Surface profile test results

Table 4.7 Average of surface profile measurements

Samples	**R_a (μm)**	**R_z (μm)**
Sample 1	5.77	50.14
Sample 2	5.88	45.94
Sample 3	5.50	53.35
Average	**5.71**	**49.81**

By referring to Table 4.7 above, the average value of surface roughness (R_a) is 5.71 (μm), while the average surface roughness depth (R_z) is 49.81 (μm). The accepted value for surface roughness is more than 2.5 μm (usually the value is between 5 to 6.5 μm, while the accepted value for surface roughness depth is in the range of 35-70 μm. The results show that both values of surface roughness and surface roughness depth are in the acceptable range.

Since all the values meet the standard requirement of the surface profile test, the coating process can be carried out. Achieving a specific value of surface roughness is a very crucial issue. Other than indicating whether or not various coatings can be applied to the cleaned blasted metal substrate, surface roughness is also a very important aspect, as it can be detrimental to the performance of coating materials. Roughness is a good predictor of the performance of a mechanical component. The reason for this is that, materials with an uneven surface or materials with unacceptable surface roughness values may form nucleation sites for cracks or corrosion. .

4.3 Salt Spray Test

The performance of all samples was evaluated by performing the salt spray test in which samples were exposed to a corroding environment in the salt spray cabinet for 720 h (30 days). All coated samples that were used as testing panels were scribed to expose the underlying metals to the environment.

Figures 4.14, 4.15 and 4.16 show the images of all samples before and after being exposed to the salt spray test. As expected, there were significant amount of rusts and

blistering on all the tested panels. The corrosion products formed during the corrosion process are mainly localized in the scribe. Also, for all samples, it was observed that the corrosion products appeared not just at the scribed areas, but around the scribed areas too.

For samples cured at room temperature (Figure 4.14), blisters on the scribed areas were found on all samples. Delamination of the coating was determined as the cause of corrosion in those areas. As a result, it also caused rusting to occur throughout the scribed areas under the film coating and also at the bottom part of the samples. The condition for every sample was observed to be almost the same. However, least occurrence of blistering, delamination and rusting for samples cured at RT were observed for sample A followed by samples B and C.

Likewise, similar conditions were observed for all samples cured at 120° C (Figure 4.15), which showed evidence of blistering, delamination and rusting phenomena but to a lesser degree. These samples were observed to be in a much better condition than the samples cured at RT. Sample F corroded the most compared to other samples. The delamination and rusting phenomena on sample F were the worst, while the condition of sample E is lesser than sample F, and sample D showed the least corroded, delaminated and rusted areas. Figure 4.16 showed the conditions for Blank samples (without PANI). The blistering, rusting and delamination for both Blank 1 and Blank 2 samples were worse than samples with PANI. However, Blank 2 exhibited a better condition compared to Blank 1. For uncoated sample, as can be seen, corrosion was evident.

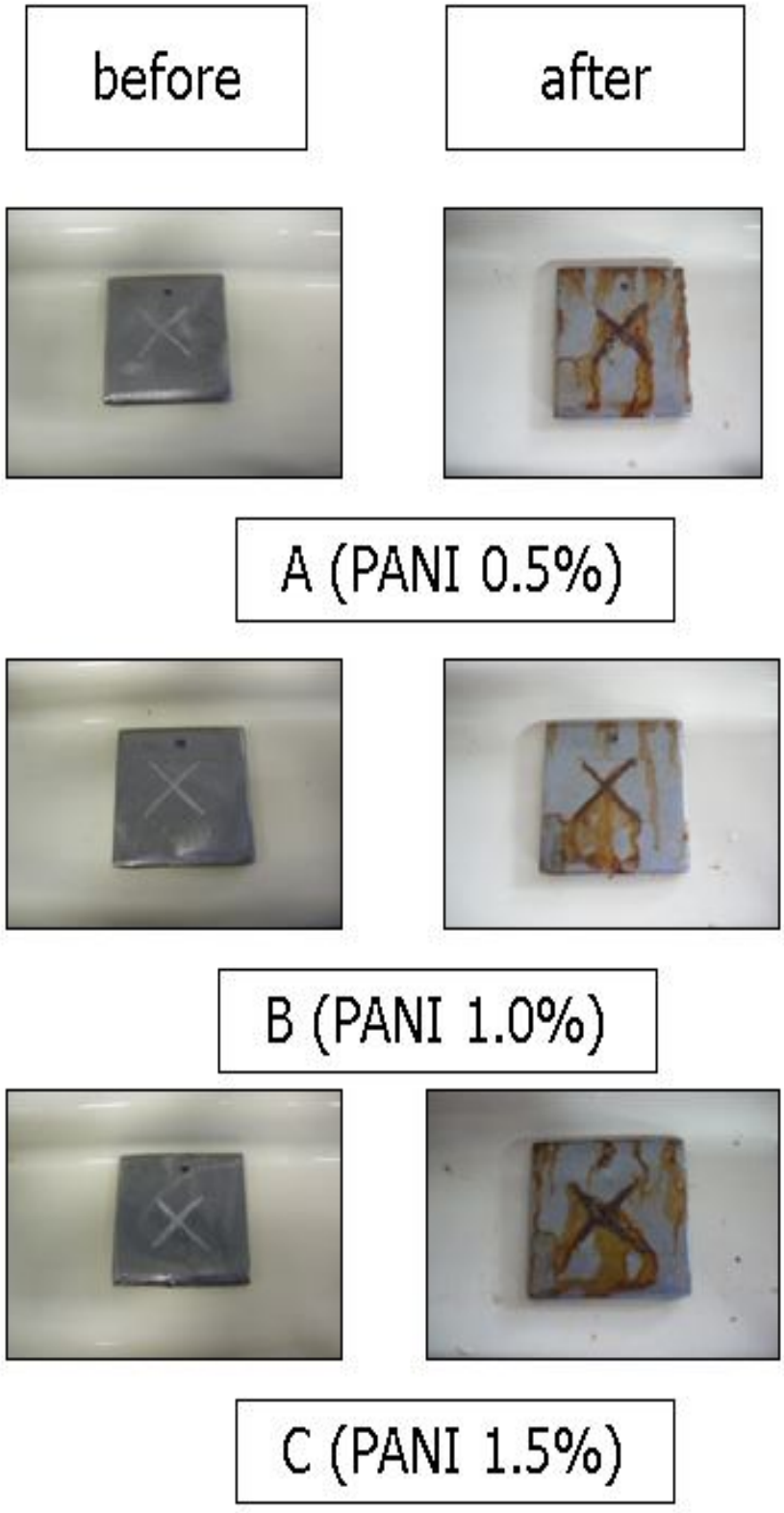

Fig. 4.14 Salt spray test results for samples cured at RT

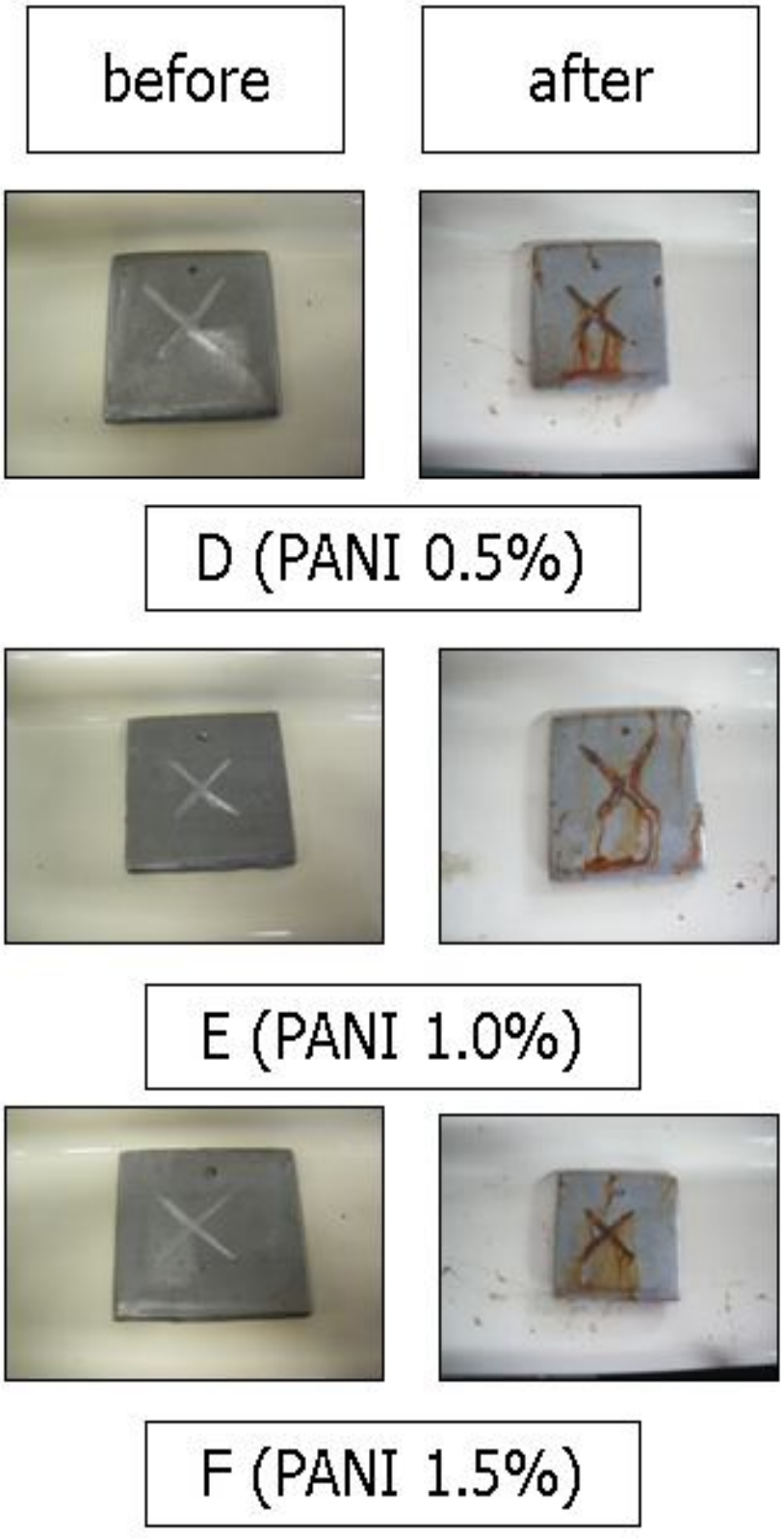

Fig. 4.15 Salt spray test results for samples cured at 120°C

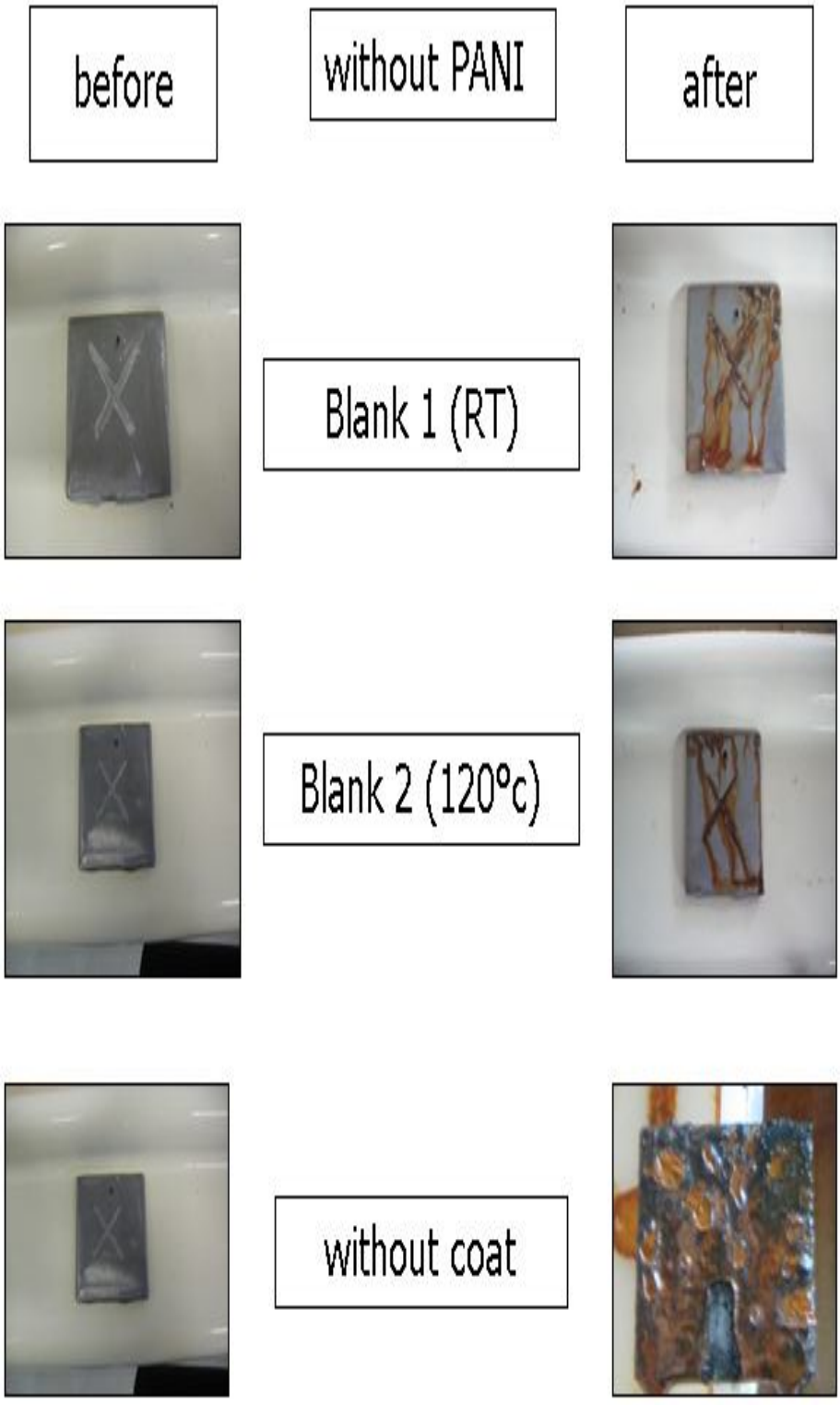

Fig. 4.16 Salt spray test results for blank and uncoated samples

Other than the visual analysis, the 720 hrs salt spray results were also evaluated in terms of delamination of the coatings. Delamination was evaluated by measuring the length of delamination from the scribed areas. Table 4.8 shows the delamination values obtained from the salt spray test and Figure 4.17 shows how the delamination was measured.

Generally, the delamination of coatings for samples cured at room temperature was higher than samples cured at 120° C including the blank samples. This is the reason why rusting and blistering that occurred on the samples cured at RT were greater and worse than samples cured at 120° C. For samples cured at RT, the delamination values increased in the order A < B < C < Blank 1, while for samples cured at 120° C, the delamination values increased in the order D < E< F< Blank 2.

Table 4.8 Performance of samples after 720 hrs of exposure during salt spray test

SAMPLE	**DELAMINATION FROM SCRIBE (mm)**
A (PANI 0.5%) – RT	4.0±2
B (PANI 1.0%) – RT	5.5±1
C (PANI 1.5%) – RT	7.0±2
D (PANI 0.5%) - 120°C	1.4±1
E (PANI 1.0%) - 120°C	2.8±3
F (PANI 1.5%) - 120°C	3.5±3
BLANK 1 (RT)	15±1
BLANK 2 (120°C)	9.0±1
UNCOATED SAMPLE	-

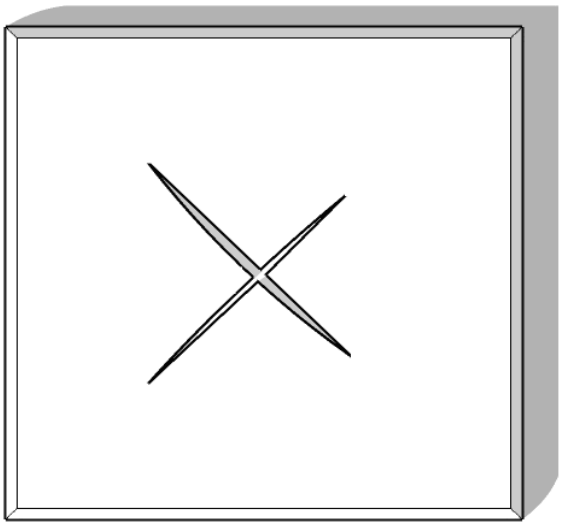

(a)

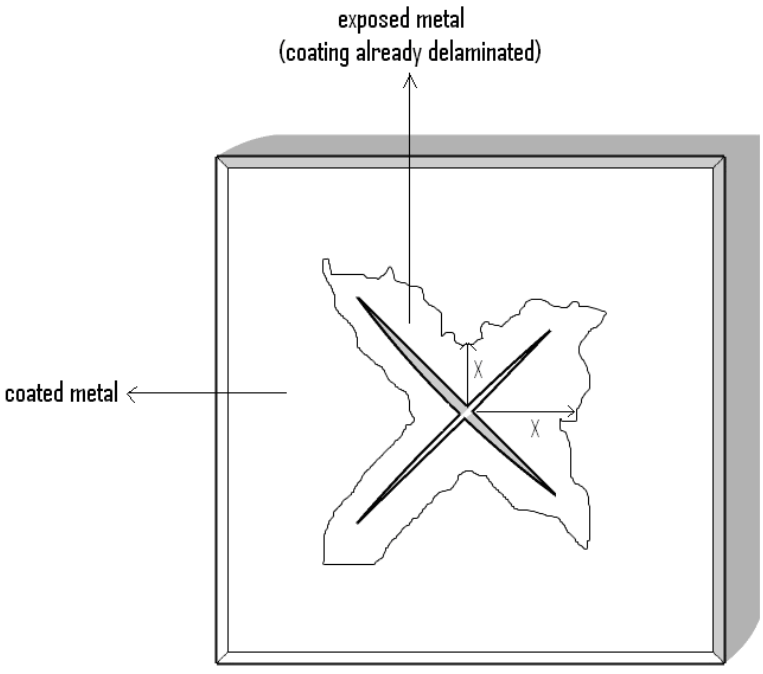

(b)

Fig. 4.17 Schematic diagrams of delamination measurement (a) coated metal without delamination (b) coated metal with some exposed metal where delamination occurred. "X" is the measured delamination values. An average of "X" is reported as the delamination value of a particular coating.

By referring to Table 4.8, the delamination value of Blank 1 sample is 15±1 mm, which is the highest value obtained among all other samples, while the lowest delamination value (1.4±1 mm) is recorded for sample D. These findings can be correlated to pull-off test results. Basically, the relationship between delamination and pull-off test is a reversible relationship. If the adhesion strength of the sample is high, supposedly there will be less delamination. In another way, it can be expressed that, a strongly adhered coating will result in less delamination. The pull-off test revealed that the adhesion strength for Blank 1 sample is the lowest, whereas the adhesion strength for sample D is the highest. This explains the lesser delamination observed on sample D compared to Blank 1 sample.

In general, based on the overall pull-off test results, the adhesion strength of all samples cured at RT are lower than the adhesion strength of all samples cured at 120°C. The adhesion strength for the blank samples is also low, with Blank 1 sample showing lower adhesion strength than Blank 2 sample. So, this is the reason for such delamination values obtained during the salt spray test. A detailed discussion on adhesion strength of the samples will be provided in the next section.

From the results obtained, it can be proposed that steels coated with PANI, particularly samples cured at 120° C, provide better corrosion protection than steels without PANI coating. It can also be concluded that samples cured at room temperature did not provide sufficient barrier to the metals as the delamination on these samples are higher than the delamination on samples cured at 120° C. These salt spray results will be supported by the results of pull-off test and morphology analysis.

4.4 Water Absorption Test

Polymeric materials such as epoxy resins are susceptible to water absorption. This is undesirable as it can cause properties degradation especially mechanical properties of the materials, which ultimately may lead to failure of the coatings [122] and [123]. Mechanical properties could be affected as absorbed moisture, which can lead to plasticization of the materials [124].

Diffusion of water into polymer has been extensively studied. Although water diffusion in epoxy resins is a complex and complicated behavior, it can be best described by the Fickian behavior (Fick's Law) [94] and [124]. If a polymer sheet is exposed to a fluid, the change of the concentration (C) of a diffusing substance as a function of time (t) and distance (x) is given by the Fick's Law (Equation 4.2) [94].

$$(\delta C/ \delta t) = D (\delta^2 C / \delta x^2) \qquad \text{Eq. 4.2}$$

Where, D is the diffusion coefficient (diffusivity). Fickian behavior has the following features: (a) at initial stages, the sorption curves are linear (M_t is proportional to $t^{1/2}$), (b) above the linear region, absorption is concaved to the abscissa and the linear region extends 60% or more of the region studied [94].

In this research, both modified and unmodified epoxy systems have been investigated with respect to their water absorption properties as a function of exposure time by running the water absorption test. Both Figure 4.18 and Figure 4.19 show the water absorption profiles for all samples cured at room temperature (RT) and 120° C respectively. Generally, the water absorption profiles for all samples, either cured at RT or 120° C, exhibit a similar trend. At the initial stage, the water gained was linearly proportional to $t^{1/2}$, which follows the Fickian behavior.

For samples cured at RT (Figure 4.18), the water absorption decreased with time in the following manner: Blank 1 > C > B > A, while for samples cured at 120° C (Figure 4.19), water absorption decreased with time in the sequence of : Blank 2 > F > E > D. After more than 500 hours, it was observed that all specimens had reached saturation. The maximum value of water gain for each sample, however, was different from one another.

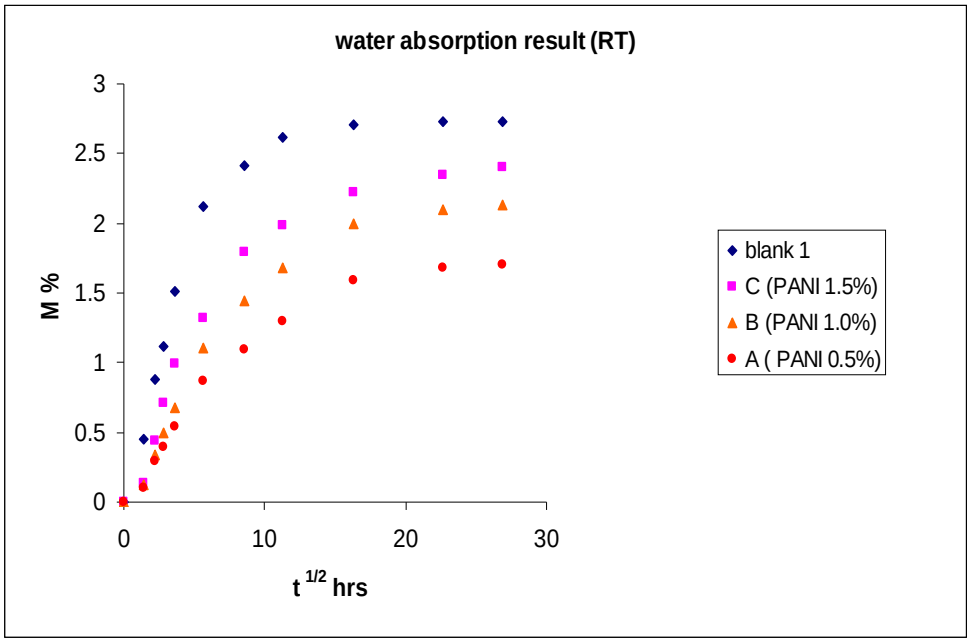

Fig. 4.18 Water absorption profile for samples cured at RT

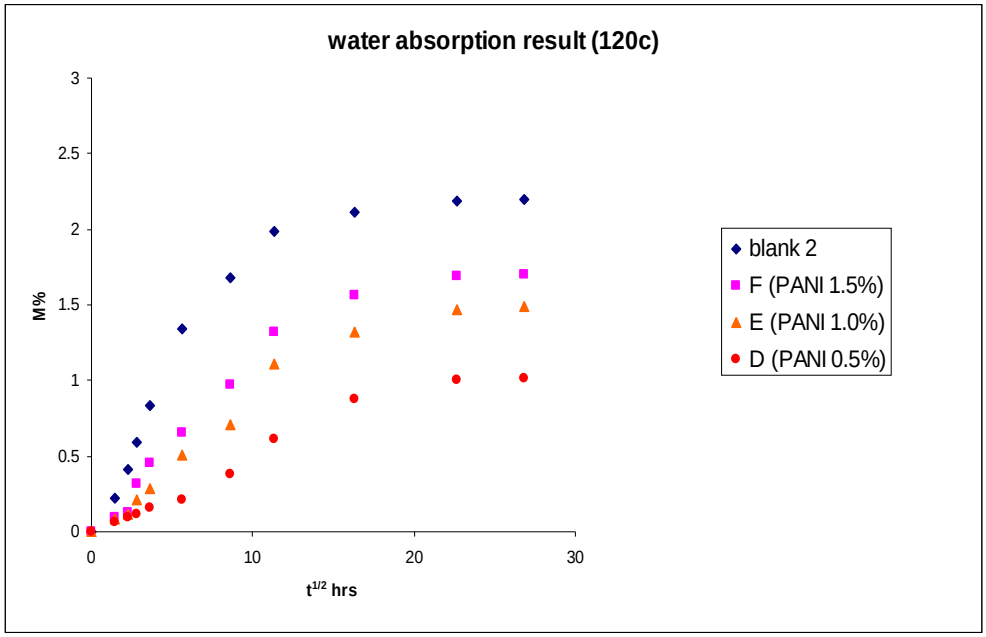

Fig. 4.19 Water absorption profile for samples cured at 120° C.

The analysis of water absorption, not only allows the determination of maximum water uptakes but also the diffusivity, D. The diffusivity, D was determined from the initial slope of the curve from the plot of the percentage of water uptake, M_t versus the square root of time, $t^{1/2}$ [94]. It can be calculated using Equation 4.3 [94].

$$(M_t / M_\infty) = (4 / h) [(Dt / \pi)^{1/2}] \quad \text{Eq. 4.3}$$

Where M_∞ is the equilibrium water uptake at saturation (maximum), h is the sample thickness and t is the exposure time. The overall values of M_∞ and D for every sample were calculated with respect to t = 128 hrs. The values are summarized in Table 4.9 below.

Table 4.9 Max. water uptake, M_∞ and diffusivity, D for all samples

SAMPLES	**MOISTURE (M_∞) %**	**DIFFUSIVITY, D (mm^2s^{-1})**
BLANK 1(RT)	2.733	1.697
A (PANI 0.5%, RT)	1.701	1.516
B (PANI 1.0%, RT)	2.130	1.540
C (PANI 1.5%, RT)	2.398	1.579
BLANK 2 (120 ^oC)	2.198	1.650
D (PANI 0.5%, 120 ^oC)	1.010	1.354
E (PANI 1.0%, 120 ^oC)	1.491	1.497
F (PANI 1.5%, 120 ^oC)	1.699	1.513

The results obtained from the water absorption test can be correlated to the values of M_∞ and D. According to Table 4.9, sample D exhibits the lowest percentage of maximum water uptake followed by sample E, F, A, B, C, Blank 2 and Blank 1. Meanwhile, the diffusivity values are in the reverse order of M_∞. The Blank 1 sample exhibits the highest diffusivity values among all, followed by Blank 2, C, B, A, F, E

and D samples. This observation suggests that higher diffusivity leads to higher amount of water being absorbed by the sample. Once again, the epoxy system containing PANI provided better protection in terms of barrier properties and is more resistant towards water absorption, and the epoxy system cured at 120° C is better than the system cured at RT.

From the results obtained, obviously, samples cured at room temperature tend to absorb more water than samples cured at 120° C. This can be related to the curing conditions of the samples. Johncock and Tudgey [92], in their studies, found that the rate of water absorption and the extent of water uptake depended on the curing temperature. Moreover, Abdelkader et al [93] claimed that one of the reasons for different amount of water absorbed by different epoxy system is due to the crosslinking effect or the extent of curing of the materials. Also, Basically, the diffusion of water into polymeric materials like epoxy systems is related to the free volume and polymer-water affinity [93]. In this case, referring to the DSC analysis results, the samples cured at RT have low values of glass transition temperature, Tg compared to the samples cured at 120° C. The analysis also revealed that the samples cured at RT were not fully reacted, and there was an excess of unreacted epoxy. This means that there are regions of high crosslink density and regions of low crosslink density in the sample. Different crosslink density regions of the material have different properties, in which a higher crosslink density resulted in lower diffusion of water as water diffusion in this region is severely hindered, while lower crosslink density resulted in higher diffusion of water [92] and [93]. A low crosslink density will result in more “holes” or free volume in the polymer structure, thus causing more diffusion of water into the system [92]. This explains why samples cured at RT absorbed more water resulting in higher maximum water uptake, M_∞ than samples cured at 120° C.

Unreacted epoxy has loose network compared to epoxy that is fully reacted. A loose network will allow the ingress of water. Water will be absorbed much easier by such system [93]. Furthermore, incomplete reaction of the cured epoxy system may produce stresses due to non-homogenous distribution of the topographical features

generated during cure. As a result, this produces “voids” in which water may cluster [93].

It can be seen that the effect of increasing PANI amount in the epoxy system, had caused different amount of water to be absorbed by the system for both curing conditions. The increase in maximum water uptake, M_∞ with increasing % of PANI is related to the degree of cure particularly the decrease of glass transition temperature, Tg values of the samples. The Tg values decreased when the amount of PANI was increased. A decreasing Tg value indicates lowering of the crosslink density.) As the crosslink density is reduced, more free volume is created in the epoxy structures, thus resulting in more water being absorbed by the system. Since the Tg of PANI decreased in the order $Tg_{PANI\ 0.5\%} > Tg_{PANI\ 1.0\%} > Tg_{PANI\ 1.5\ \%}$, it explains why 0.5% of PANI has the lowest crosslink density compared to others. That is why samples with 0.5% of PANI absorbed less water than samples with 1.0% and 1.5 % of PANI. Meanwhile, the Blank samples (contain no PANI) absorbed the highest amount of water due to the same reason. This is supported with findings obtained by Abdelkader et al. [93] which stated that the higher level of water absorption is actually related to the imperfect cure of the materials.

Another factor related to the absorption and diffusion of water into polymeric materials is polymer-water affinity. Water exists in two different environments, and usually the term usually used to describe them are “bound/unbound” and “free” water. “Bound water” is molecules bound to specific sites, while “free water” is water clustered in voids. According to Blanco et al [125], the amount of bound water is mainly dependent on the polarity of molecules while the amount of free water is determined by the network structures. Bound water that attaches to the polymer through hydrogen bonds disrupts the inter chain hydrogen bonds and induces swelling [126] and plasticizes the polymer. When the plasticizing effect becomes stronger, it subsequently leads to lowering and degradation of the mechanical properties of the materials [93].

From these findings, it can therefore be concluded that less water being absorbed by the system will result in less degradation of mechanical properties of the materials,

thus providing better protection against corrosion. These findings will be correlated to the results from wet adhesion test and water uptake determined from EIS analysis which will be discussed in the next sections.

4.5 Pull-off Test

4.5.1 Dry Adhesion

Epoxy coating works well as a protective coating. However, the barrier coating may fail over time when it is being exposed to the environment. Organic coatings have been discovered as capable of developing an “under coating corrosion” which initiates from weak spots and develops into blisters leading to corrosion failure. The failure of organic coatings is known as delamination [46].

One of the factors that lead to delamination is the absorption of water through the coating. Water is known to have the tendency to accumulate at the interface, thereby replacing the bonds that exist between the metal and polymer, eventually resulting in the loss of adhesion [127]. Therefore, adhesion plays an important role in the protection of metals. A strongly adhered coating may help to prevent metals from delamination, thus preventing corrosion.

In this research, the adhesion of coating to the metallic substrate was investigated by performing pull-off tests. The adhesions of all samples were evaluated in terms of force that needs to be applied in order to detach the test dollies adhered to the coatings from the underlying metals. The adhesion values obtained from the test are tabulated in Table 4.10 and the trend of the results is as shown in Figure 4.20.

The adhesion strength for Blank 1, A, B and C samples which were cured at room temperature were 310± 9, 530± 1, 430± 3 and 410± 4 psi respectively. Sample A has the highest adhesion strength while the Blank 1 sample exhibits the lowest adhesion strength among all. The adhesion strength decreases in the sequence: A> B> C> Blank 1. Meanwhile, for Blank 2, D, E and F samples cured at 120° C, the adhesion strength recorded for them was 400± 4, 730± 2, 580± 5 and 510± 7 psi, respectively.

Just like samples cured at RT, sample with 0.5% PANI content (sample D) also exhibits the highest value of adhesion strength and sample without PANI (Blank 2) exhibits the lowest value. The adhesion strength for samples cured at 120^{o} C decrease in the same order as samples cured at room temperature: D>E>F>Blank 2.

Table 4.10 The dry adhesion strength values of samples for both curing conditions

CONDITION		Adhesion strength (psi)
RT		
	BLANK 1	310± 9
	A (PANI 0.5%)	530± 1
	B (PANI 1.0 %)	430± 3
	C (PANI 1.5%)	410± 4
120°C		
	BLANK 2	400± 4
	D (PANI 0.5%)	730± 2
	E (PANI 1.0%)	580± 5
	F (PANI 1.5%)	510± 7

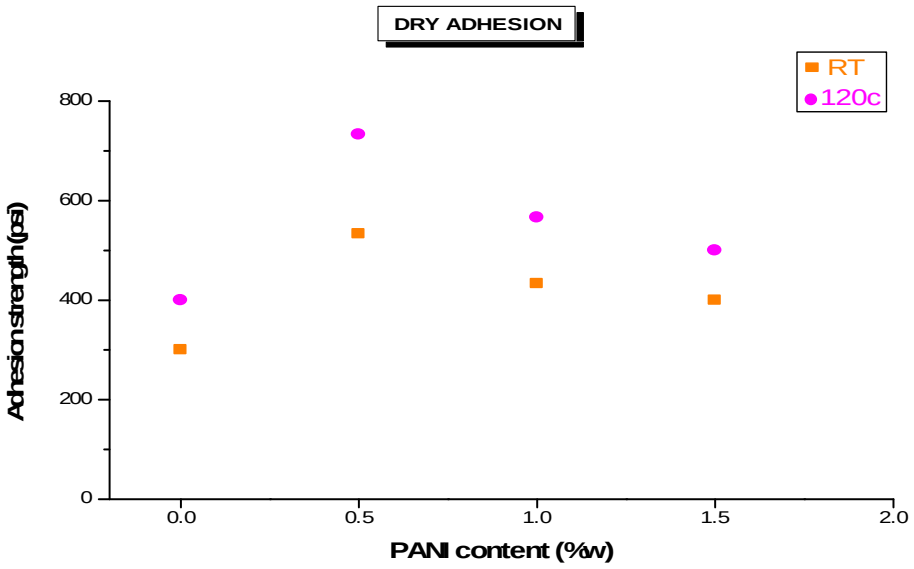

Fig. 4.20 The trending of dry adhesion strength values for both curing conditions

Comparing the adhesion strength results of all samples from both curing conditions, in general, all samples cured at 120° C exhibit better values of adhesion strength compared to samples cured at room temperature, while sample D has the highest adhesion strength among all. This finding can be correlated to higher water absorbance by samples cured at room temperature (including blank 1 sample) , obtained from the water absorption analysis as discussed in section 4.4.

The crosslinking of polymeric materials has a significant effect on the adhesion of polymer to metals. Polymers with higher glass transition temperature, Tg have better barrier (adhesion) property, thus reducing the diffusion of ions into the polymeric coatings [75]. This explains why such adhesion strength results were obtained for each sample. Those results are in correlation with their glass transition temperature (Tg) values obtained from the DSC analysis. For instance, sample D has the highest adhesion strength because the Tg value of sample D is also the highest compared to other samples. All samples cured at RT have lower adhesion strength than samples cured at 120° C because the samples were not fully cross-linked, as indicated by the low Tg values.

Although samples with the incorporation of PANI show higher adhesion strength values than the blank samples, the adhesion strength decreased when the amount of PANI was increased. When the amount of PANI was increased, the coating seemed to be less adhered to the metal substrate. However, there was not much difference regarding the adhesion strength value every time the PANI content was being increased (PANI 0.5% - PANI 1.5%). The decrease of adhesion strength caused by the increment of PANI amount has not been investigated so far and further studies are needed to elucidate the reaction involved.

The higher the adhesion strength means that the higher the forces needed to detach the coating from the metal as the coating is strongly adhered to the metal. So, it can be propose that, a highly adhered coating to the metal substrate will result in better barrier effect. Better barrier property will restrict the diffusion of water and other ionic species and therefore preventing the metals from corrosion. In this case, sample D which was highly adhered to the substrate compared to other samples, is

expected to show better corrosion protection. This will be supported and correlated with other tests results in other sections.

4.5.2 Wet Adhesion

Upon exposure to water, the adhesion between the coating and the metal substrate will be rapidly lost and water will accumulate at the interface [127]. The wet adhesion test was performed to determine the adhesion of the coatings after being exposed to water. It was performed right after the samples were being immersed in the water bath for 30days.

Table 4.11 and Figure 4.21 indicate the adhesion strength values and trending for wet adhesion of the coatings. For samples cured at room temperature, the adhesion values for Blank 1, A, B and C samples were 270± 5, 470± 5, 370± 2 and 350± 3 psi respectively. The adhesion strength values decreased in the sequence similar to dry adhesion in which A > B> C> Blank 1. For samples cured at 120° C, the adhesion values for Blank 2, D, E and F samples were determined to be 380± 3, 670± 3, 480± 2 and 450± 4 psi respectively. The adhesion strength values also decreased in the same order as dry adhesion where sample D >E > F> Blank 2.

By comparison with dry adhesion, there were slight decrements of the adhesion values for every sample for both curing conditions after being exposed to water. These findings can be well correlated to the water absorption test. The test indicated that the percentage of water absorbed by samples cured at room temperature increased in the following maner: Blank 1>C >:B>A and for samples cured at 120° C, the percentage of water increased in the sequence: Blank 2 > F> E > D. These water absorption test results explain why the adhesion strength decrement occurred.

In this case, by taking sample D for example, it can be well explained that sample D exhibit the highest wet adhesion strength value simply because it absorbed the lowest amount of water during the exposure to water. From the water absorption test result, the percentage of water absorbed by sample D was 0.107% which was the lowest percentage among all the other samples. As discussed earlier, the absorption of

water will weaken the adhesion of the coating to the metal substrate. The hydrogen bonds between the coating and metal surface has been displaced by water.

Table 4.11 The wet adhesion strength values of samples for both curing conditions

CONDITION		Adhesion strength (psi)
RT		
	BLANK 1	270± 5
	A (PANI 0.5%)	470± 5
	B (PANI 1.0%)	370± 2
	C (PANI 1.5%)	350± 3
120°C		
	BLANK 2	380± 3
	D (PANI 0.5%)	670± 3
	E (PANI 1.0%)	480± 2
	F (PANI 1.5%)	450± 4

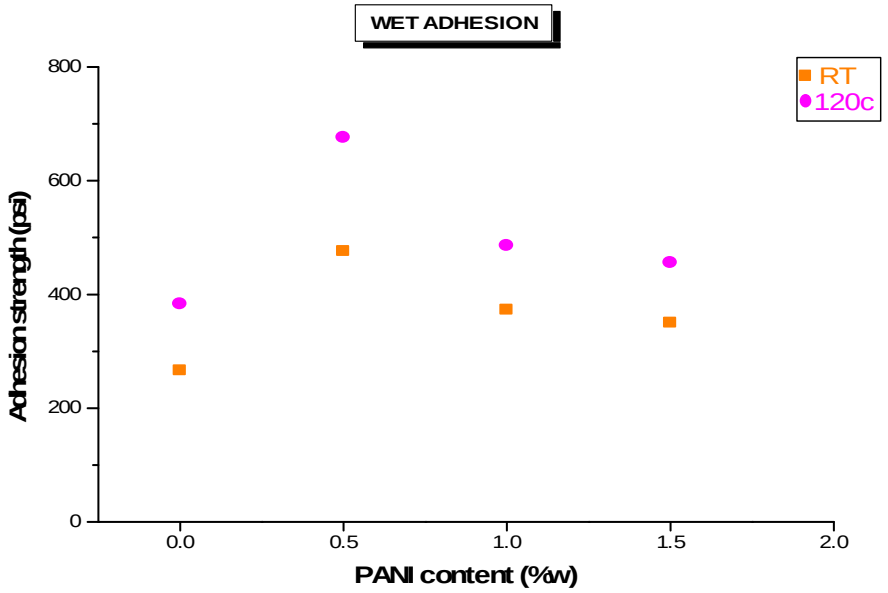

Fig.4.21 The trending of wet adhesion strength values for both curing conditions

In general, the adhesion strength values for all coatings can be accepted. The minimum requirement of adhesion strength values needed by most applications is usually above 200 psi. The adhesion strength values obtained for all coatings were greater than 200 psi. It shows that the epoxy systems are capable of providing good adhesion properties to all the samples. However, coatings with PANI (A-F) exhibit higher values of adhesion strength than coatings without PANI (Blank 1 and Blank 2) in which this indirectly proved that PANI also improves the adhesion strength of the coatings.

From the results obtained for both dry and wet adhesion, few conclusions can be made. Sample with the highest adhesion strength value will provide better corrosion protection to the metal substrate. Better adhesion will prevent the process of delamination thus avoiding corrosion phenomena. These findings will be correlated with the images obtained from morphology analysis by digital microscope which will be discussed in the next section.

In addition, adhesion is a very complex issue as there are many factors that influence the adhesion of a coating. What matter most is how to maintain the durability of the adhesion in order to attain good performance of the coatings towards corrosion protection. The durability of the coatings was determined by the salt spray and EIS tests results as discussed in section 4.3 and 4.6.

4.6 Electrochemical Impedance Spectroscopy (EIS)

The corrosion behavior of coatings (with and without Polyaniline) on steel has been determined by measuring the impedance characteristics in 3% NaCl for 30 days (720hrs). The Nyquist plots obtained from the impedance measurement for all the samples are shown in Figures 4.22 -4.24.

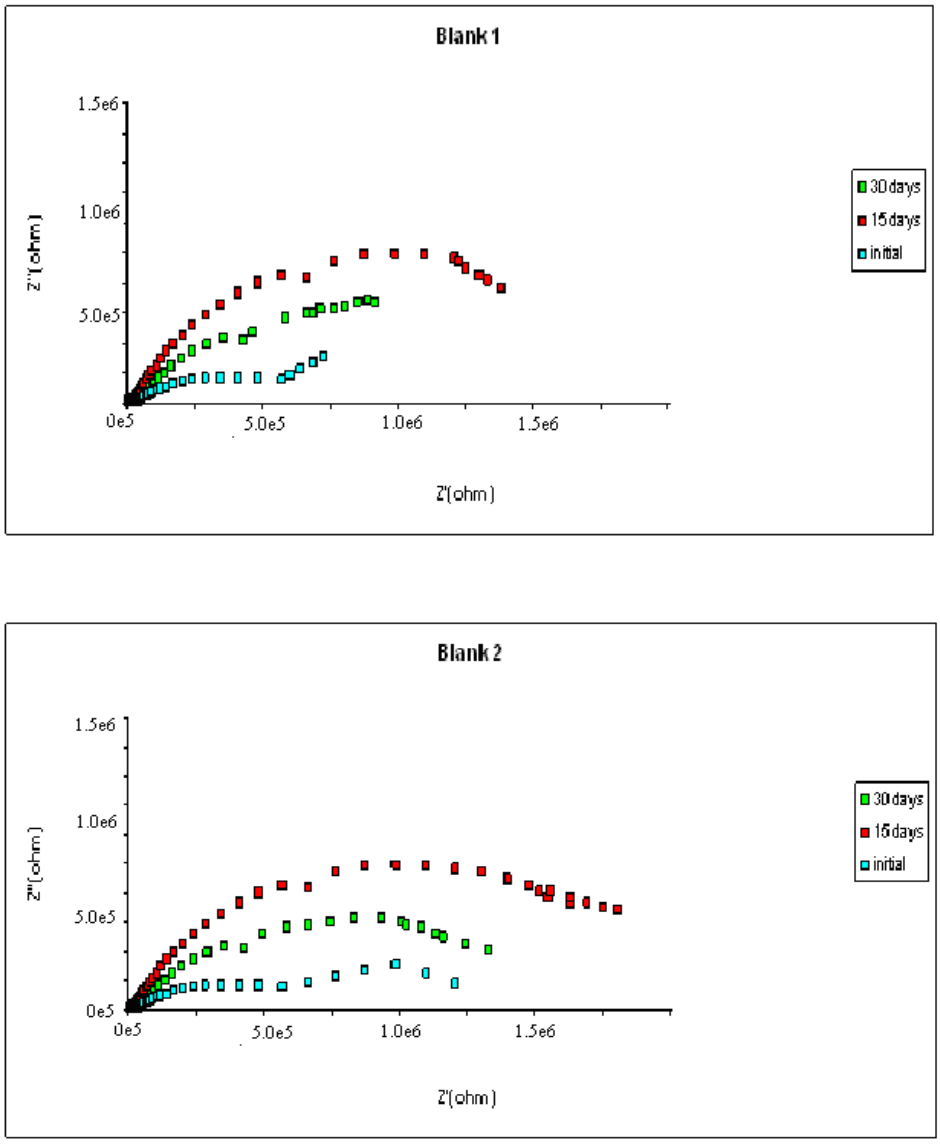

Fig. 4.22 Nyquist diagrams obtained for Blank 1 and Blank 2 samples after 30days immersion in 3% NaCl.

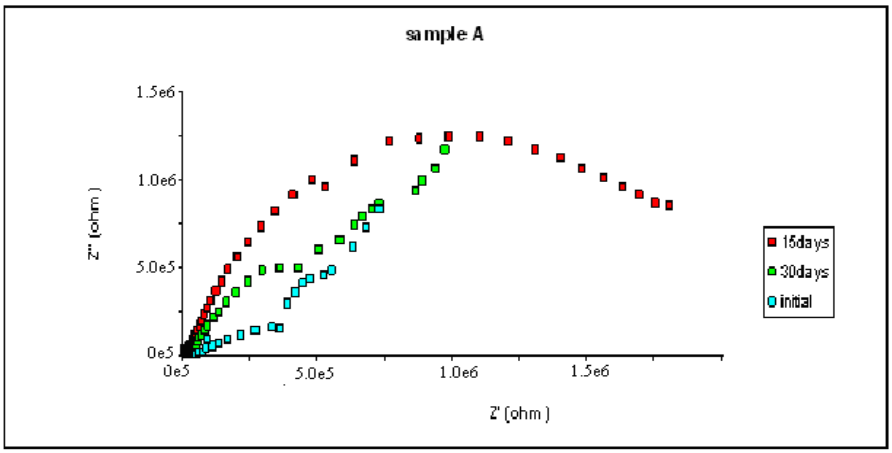

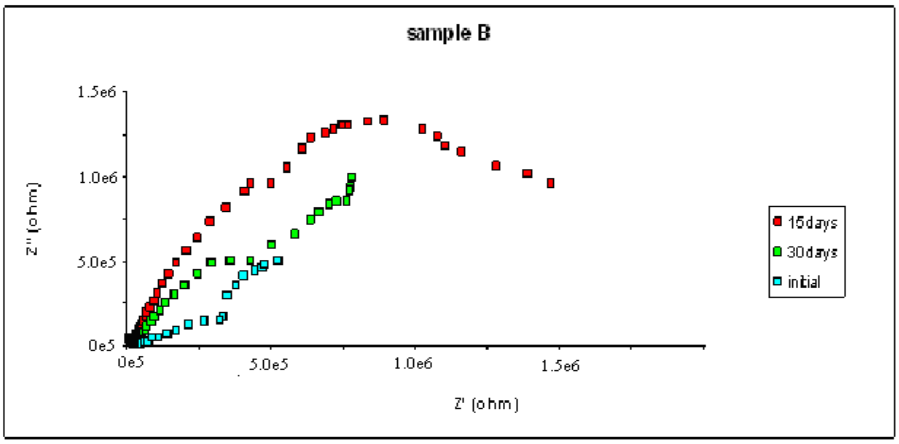

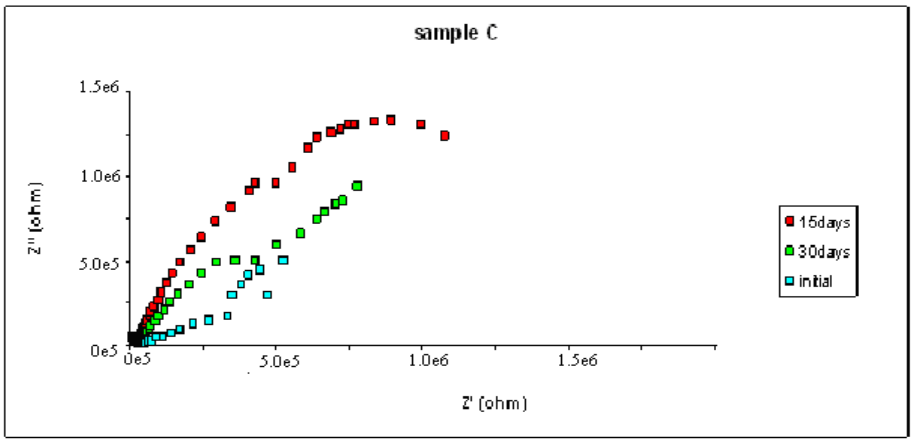

Fig.4.23 Nyquist diagrams obtained for samples A, B and C after 30days immersion in 3% NaCl.

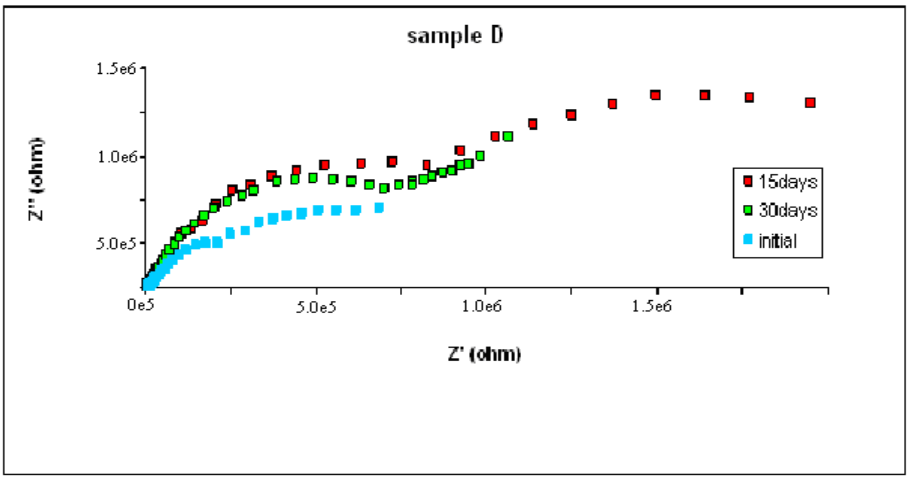

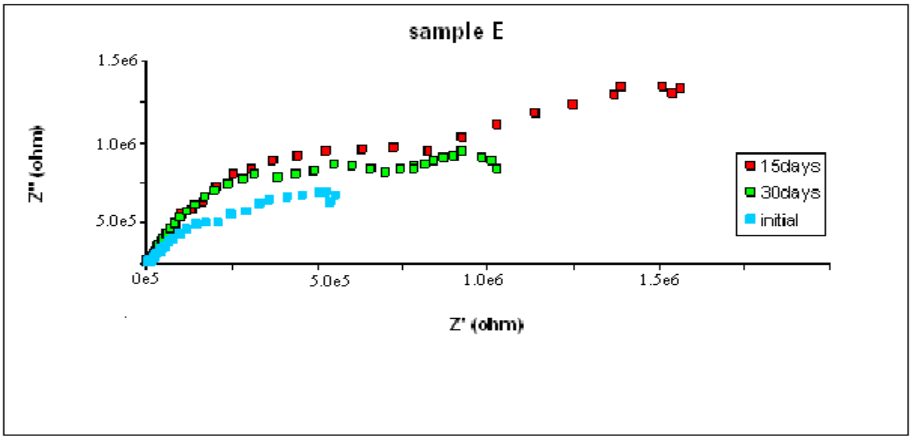

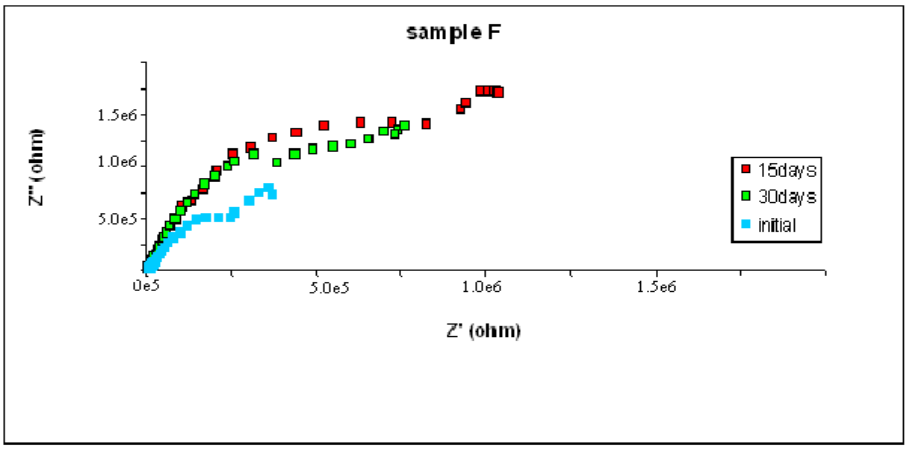

Fig. 4.24 Nyquist diagrams obtained for samples D, E and F after 30days immersion in 3% NaCl

Generally, the Nyquist diagrams show two loops: a smaller one at high frequency, followed by a larger one at the low frequency range. The smaller loop is attributed to the characteristics of the coatings in which it actually relates to the charge transfer resistance of the coating (Rct), while the larger loop is related to the process occurring underneath the film [58] and [105]. The equivalent circuit that usually represents these types of electrochemical behaviors is shown in Figure 4.25

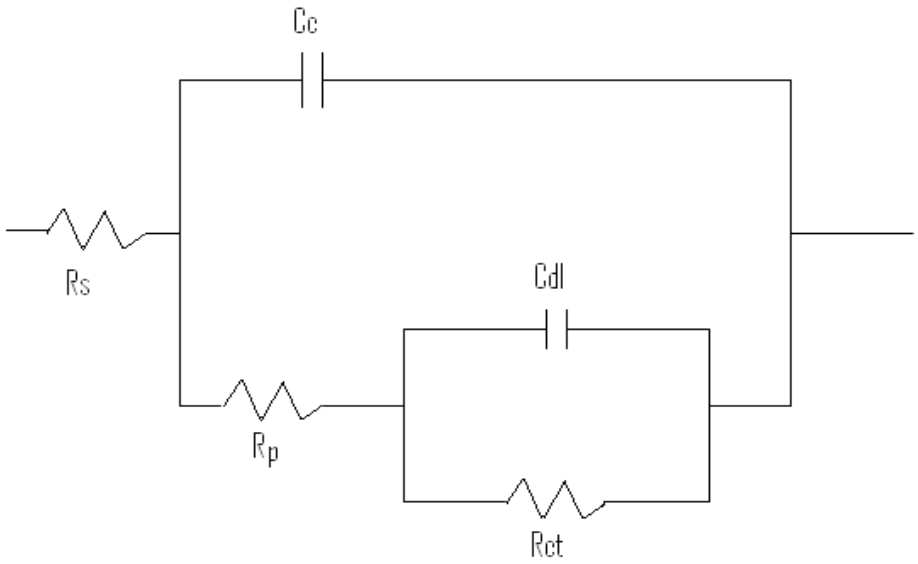

Fig. 4.25 Equivalent circuit to simulate the impedance test

By referring to the above circuit, R_s, R_p, C_c, R_{ct} and C_{dl} correspond to the solution resistance, the coating resistance, the coating capacitance, the charge transfer resistance and the double layer capacitance respectively. The impedance parameters for the above equivalent circuit were obtained from the FRA software. The values of each parameter for all samples are summarized in Table 4.12.

From the data obtained, it can be seen that all samples cured at 120° C (D, E, F and Blank 2) has higher initial coating resistance, Rp than samples cured at room temperature (A,B, C and Blank 1). Sample D exhibits the highest value of Rp among all samples while Blank 1 exhibits the lowest value of Rp. It can be suggested that initially, samples with epoxy/PANI system have higher resistance than samples with only epoxy (without PANI) system.

Table 4.12 Impedance data obtained by simulation of the results in Fig. 4.22-4.24

Samples	Time (days)	Rp (x $10^5\Omega$)	Cc (10^{-9} F)	Rct(x 10^5 Ω)	Cdl (10^{-9})
Blank 1	**initial**	0.67	0.99	0.52	1.85
	15	1.11	0.43	1.28	0.95
	30	0.79	0.79	0.71	1.34
Blank 2	**initial**	1.30	1.11	1.39	2.98
	15	1.92	0.66	2.01	2.20
	30	1.63	0.87	1.56	2.74
Sample A	**initial**	3.62	1.87	4.83	5.72
	15	4.14	1.70	5.62	5.21
	30	3.89	1.77	5.11	5.36
Sample B	**initial**	2.97	1.75	3.45	4.90
	15	3.55	1.62	4.44	3.45
	30	3.12	1.70	3.97	4.15
Sample C	**initial**	2.09	1.72	2.49	4.66
	15	2.61	1.41	3.19	3.12
	30	2.22	1.59	2.76	4.07
Sample D	**initial**	5.91	2.34	7.89	6.68
	15	6.21	2.20	8.44	6.20
	30	6.04	2.28	8.12	6.31
Sample E	**initial**	5.09	2.11	7.05	6.12
	15	5.83	1.99	7.69	6.01
	30	5.21	2.03	7.41	6.09
Sample F	**initial**	4.19	2.04	5.81	5.93
	15	4.77	1.79	6.78	5.59
	30	4.42	1.81	6.10	5.87

By taking sample D as an example, it was observed that the coating resistance, R_p increased gradually from 591 kΩ to 621 kΩ cm^2 after 15 days of immersion. This shows that the protective property of the coating has increased [58], [66], [105] and [107]. In addition, the decreased of coating capacitance, C_c from 2.34 to 2.2 nF/cm^2 also occurred for the same reason.

On the other hand, the increase of charge transfer resistance, R_{ct} for sample D from 789 to 844 kΩ cm^2 and the decrease of the double layer resistance, C_{dl} from 6.68 to 6.20 nF cm^2 proved that dissolution of iron under the film was negligible during the 15 days of immersion and also indicating the corrosion stability of this protective system [107]. The reduction of C_{dl} is actually the result of the subsequent formation of a passive layer. The same conditions were observed for other samples. The coating resistance, R_p of each sample decreased in the following order: R_p D > R_p E > R_p F >R_p A > R_p B > R_p C> R_p Blank 1 > R_p Blank 2. It can be concluded that sample D is more resistant towards corrosion compared to other samples for the first 15 days of immersion in 3% NaCl.

However, different findings were obtained when immersion time reached 30 days. After 30 days, the corrosion resistance, R_p for sample D decreased from 621kΩ to 604kΩ while the corrosion capacitance C_c was observed to have increased from 2.2nF/cm^2 to 2.28nf/cm^2. These conditions indicate that there was a reduction in the protective properties of the coatings. Meanwhile, a slight decreased of charge transfer resistance, R_{ct} value from 844 kΩ cm^2 to 812 kΩ/cm^2 and an increase in the value of double layer capacitance, C_{dl} from 620 nF/cm^2 to 631 nF/cm^2 of sample D have also been determined when reaches the 30^{th} day of immersion.

The changes of R_p, C_c, R_{ct} and C_{dl} values indicate that there were changes of behavior of the protective properties. The decrease of R_{ct} value indicates that there may be due to small amount of dissolution of iron and the degradation of the passive oxide layer formation. This is supported with the increase of C_{dl} value of the coating in which the increase of C_{dl} is actually due to the delamination of the coating. The double layer capacitance actually illustrates the disbanding of the coating and the under film corrosion [23]. Moreover, in most coatings, the decrease of resistance and the increase of capacitance values are due to the ingress of water or chloride ions. So,

based on the results obtained from this study, it is expected that after 15 days, there was a small dissolution of iron and delamination of coating occurred in which this resulted in the water being absorbed by the coating.

Similar conditions were also observed in other samples. However, sample D still remain to be more resistant towards corrosion compared to other samples even after 30 days of immersion. The coating resistance, Rp decrease in the following manner: R_p Blank 1 < R_p Blank 2 < R_p C <R_p B < R_p A < R_p F < R_p E < R_p D.

The charge transfer resistance, R_{ct} which indicates the kinetic properties of the coating is inversely proportional to the corrosion rate [58]. The decrease of R_{ct} for sample D after 30 days of immersion indicates that higher corrosion rate was obtained by the sample. The values of corrosion rate can be determined by using the Stern-Geary Equation (4.4a) and Faraday's Law (4.4b):-

$$i_{corr} = \frac{\beta}{Rp} \qquad \text{Eq. 4.4a}$$

$$corrosion\ rate = \frac{i_{corr}\ A}{nF\rho} \qquad \text{Eq. 4.4b}$$

Where, β is Tafel constant (25), Rp is the polarization resistance, A is the atomic or molecular weight, g/mol (Fe = 56), n is the number of electrons transferred in the half cell reaction in which n= 2, ρ is the density of specimen (Fe = 7.86 g/cm3) and F is the Faraday constant (96485 C/mol).

The value of i_{corr} can actually be obtained directly from other EIS analysis such as the Tafel slope or linear polarization measurement. However for impedance measurement, i_{corr} can still be obtained by using Eqn. 4.4a. The value of R_p is equal to the value of charge transfer resistance, R_{ct}. By knowing the i_{corr} values, the corrosion rate values for all samples can be determined by using Equation 4.4b. The overall values of corrosion rate for all samples obtained from the impedance measurement are tabulated in Table 4.13.

Table 4.13 The values of i_{corr} and corrosion rates for all samples

Samples	Time (days)	R_{ct}	i_{corr}	corr. rate (g/cm^2s)
	0	5.20E+04	4.81E-04	1.78E-08
Blank 1	**15**	1.28E+05	1.95E-04	7.21E-09
	30	7.10E+04	3.52E-04	1.30E-08
	0	1.39E+05	1.80E-04	6.64E-09
Blank 2	**15**	2.01E+05	1.24E-04	4.59E-09
	30	1.56E+05	1.60E-04	5.92E-09
	0	4.83E+05	5.18E-05	1.91E-09
Sample A	**15**	5.62E+05	4.45E-05	1.64E-09
	30	5.11E+05	4.89E-05	1.81E-09
	0	3.45E+05	7.25E-05	2.68E-09
Sample B	**15**	4.44E+05	5.63E-05	2.08E-09
	30	3.97E+05	6.30E-05	2.33E-09
	0	2.49E+05	1.00E-04	3.71E-09
Sample C	**15**	3.19E+05	7.84E-05	2.89E-09
	30	2.76E+05	9.06E-05	3.34E-09
	0	7.89E+05	3.17E-05	1.17E-09
Sample D	**15**	8.44E+05	2.96E-05	1.09E-09
	30	8.12E+05	3.08E-05	1.14E-09
	0	7.05E+05	3.55E-05	1.31E-09
Sample E	**15**	7.69E+05	3.25E-05	1.20E-09
	30	7.41E+05	3.37E-05	1.25E-09
	0	5.81E+05	4.30E-05	1.59E-09
Sample F	**15**	6.78E+05	3.69E-05	1.36E-09
	30	6.10E+05	4.10E-05	1.51E-09

\

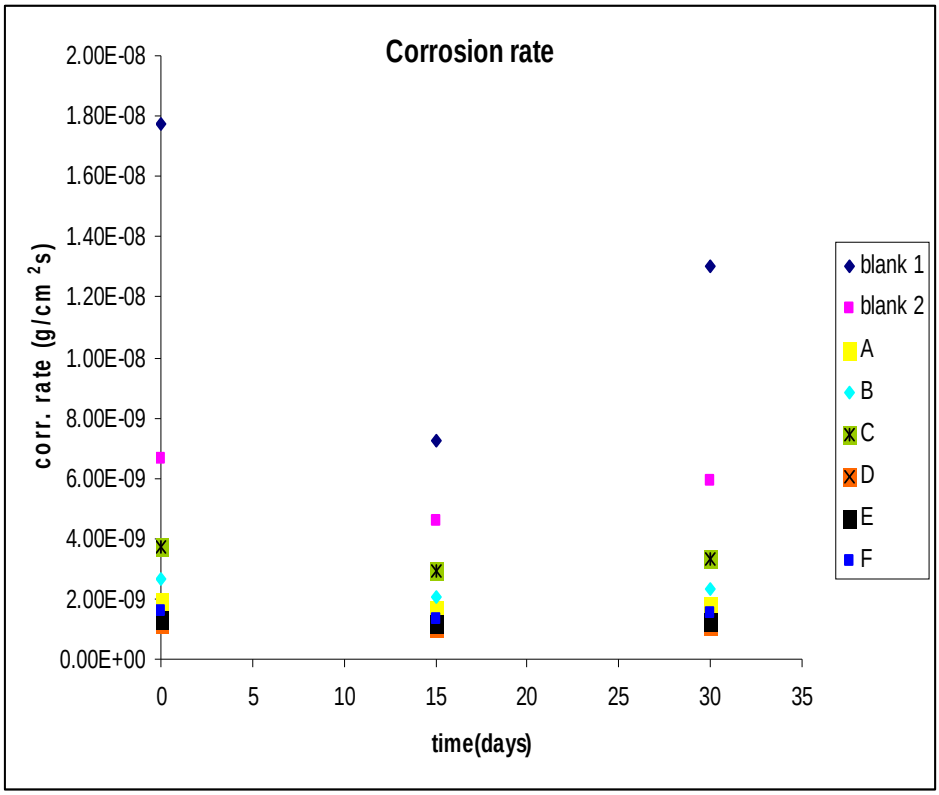

Fig. 4.26 The trending of corrosion rate values for all samples

In general, it can be seen from the table above that all samples exhibit certain values of corrosion rate (in nano level) initially. After 15 days of immersion, the corrosion rates for all samples have slightly dropped compared to the initial. For example, the initial value of corrosion rate for sample D was 1.17e-9 g/cm2s but it has decreased to 1.09e-9 g/cm^{2}s after 15 days of immersion in NaCl. This is in agreement with the changes of all parameters (R_p, C_c, R_{ct} and C_{dl}) obtained from the impedance measurement.

The reduction of corrosion rate can be correlated to the increase of coating resistance, decrease of coating capacitance, increase of charge transfer resistance and decrease of double layer capacitance. The increase of the charge transfer resistance has proven that there was a formation of a protective oxide layer, in which this layer has contributed to the decrease of the double layer capacitance thus decreasing the rate of corrosion of the coating.

However, as the immersion time reached 30 days, the corrosion rates for all samples increased. The charge transfer resistance also decreased which revealed the breakdown of the passive oxide layer on the metal surface. As a result, water may passes through the coating and caused the distribution of ionic charges around the unprotected metal resulting in the increase of the double layer capacitance values [58], [66], [105] and [107].

From the corrosion rate values obtained, it can be concluded that each coating (except Blank samples) has stable protective oxide layer up to 15 days of exposure to 3% NaCl. However, the protective oxide layer is expected to have deteriorated causing the increase of corrosion rate after 30 days immersion and this is supported with the increase of the C_{dl} values. All samples cured at 120° C exhibits lower corrosion rates compared to samples cured at RT. In addition, samples without PANI (Blank samples) exhibit the highest value of corrosion rates than samples with PANI. This could be due to the non-protective oxide layer that could be produced by coating systems without PANI.

Although the coating resistance of all samples decreased after 30 days of immersion, the capacitance and resistance values obtained for all samples remain in the ranges characteristics for an intact coating with excellent barrier properties. In addition, there were no linear portions have been observed in the low frequency regions at later periods throughout the immersion time. This indicates that no Warburg impedance occurred. Therefore, it can be suggested that there's no diffusion of ions or molecules along the polymer pores in which this indicated that all coating systems are depended on diffusion control [128].

4.6.1 Proposed Protection Mechanism by PANI

In general, PANI confers protection by exchanging electrons with the metallic substrate. It has been postulated that the electrically conductive polymer stabilizes the potential of metal in the passive regime, maintaining a protective oxide layer on the metal. Oxygen reduction on the polymer coating is thought to replenish the polymer charge consumed by the metal dissolution, thereby stabilizing the potential of the base metal in the passive region and minimizing the rate of metal dissolution [65].

In this case, judged from the changes of all the parameter (Rp, Cc, Rct, Cc) obtained via the impedance measurement, the main reactions during the initial period of immersion can be related to the mechanism proposed by Kinlen et al [37] as mentioned earlier in Chapter 2. This protection mechanism happened could be explained by first considering the anodic and cathodic reactions that happened at the metal / polymer interface.

Anodic reactions:-

1. oxidation of iron (Fe) occurred : $2Fe \rightarrow Fe^{2+} + 4e$
2. reduction of PANI : Emeraldine salt $\rightarrow$ Leucoemeraldine + (DOP^-)).

The anodic reactions were coupled with cathodic reactions that took place at the polymer/solution interface, where:-

Cathodic reactions:-

1. $O_2 + 2H_2O + 4e \rightarrow 4\ OH^-$
2. Leucoemeraldine + $(DOP^-) \rightarrow$ Emeraldine salt

The redox reactions were assumed to happen at the polymer/metal interface in which it subsequently leads to the formation of iron/DOP complex $(FeODOP)^-$ as shown in Figure 4.27. This complex formed is the oxide layer that protects the metal from undergoing further corrosion.

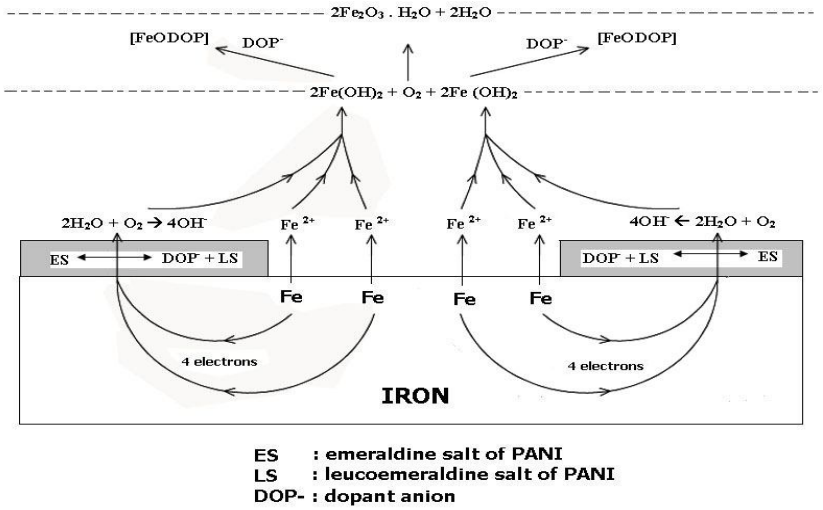

Fig. 4.27 Protection mechanism proposed (Adapted from Kinlen [37])

The formation of this protective oxide layer may be the reason for the increase of the coating resistance, Rp and coating capacitance, Cc after 15 days of immersion. Since the metal is protected by the oxide layer, less charge is "allowed" to be transferred at metal/solution interface. Therefore the increase of charge transfer resistance, Rct and the decrease of double layer capacitance, Cdl were observed.

On the other hand, it was observed that the coating resistance, Rp values decreased and the coating capacitance, Cc increased after 30 days of immersion. It is expected that the protective properties of the PANI oxide layer has dropped. As a result, it also caused the charge transfer resistance, Rct to decrease. A highly charge transfer occurred between the metal and protective oxide layer and this result in the increase of capacitance double layer, Cdl to increase.

4.7 Morphology Analysis

Microscopic observations of all the coatings were implemented by using the digital microscope to determine the regularity in the surface of the coatings as well as to identify the possible failures that may give place to corrosion. The digital micrographs of the coatings before and after 30 days immersion in 3% NaCl are shown in Figure 4.28-4.30.

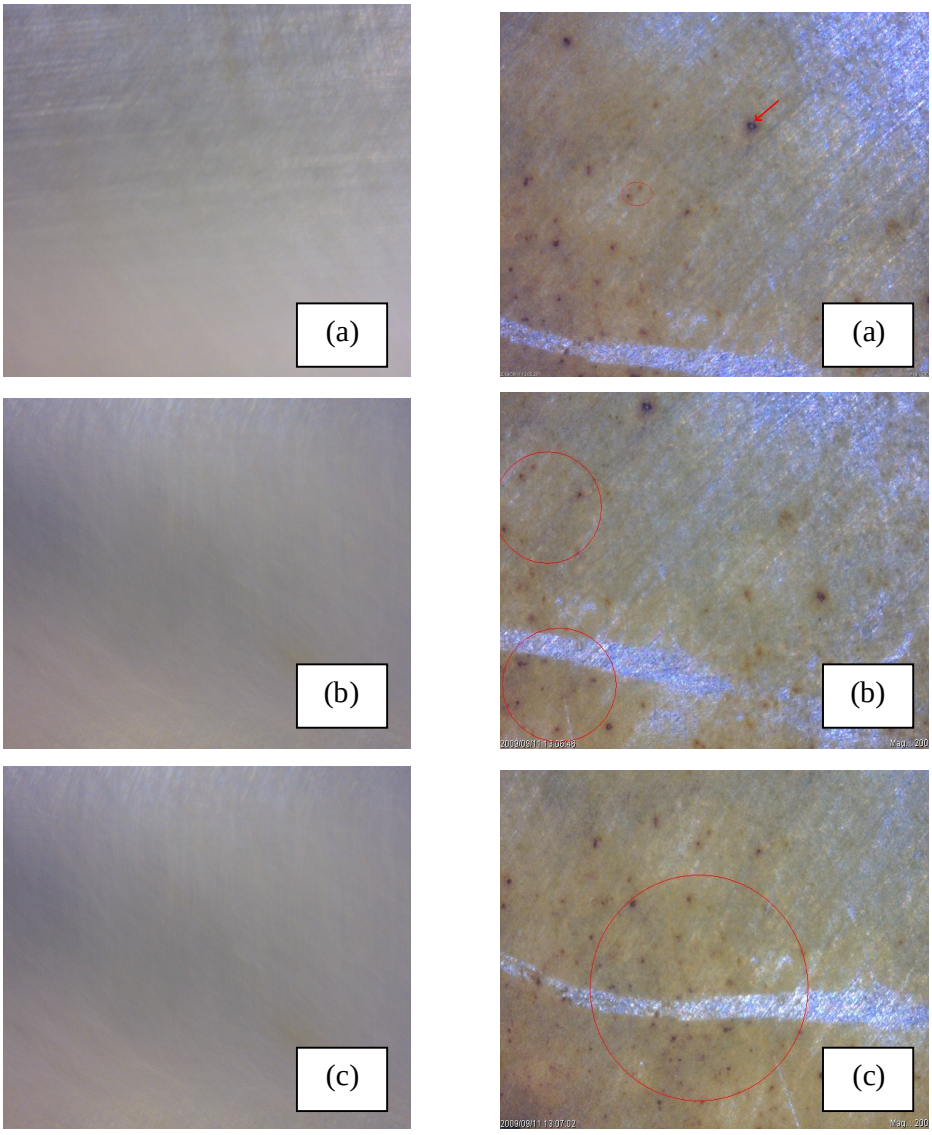

Fig. 4.28 Digital micrographs before (left) and after (right) 30days immersion in NaCl for sample (a) A, (b) B and (c) C.

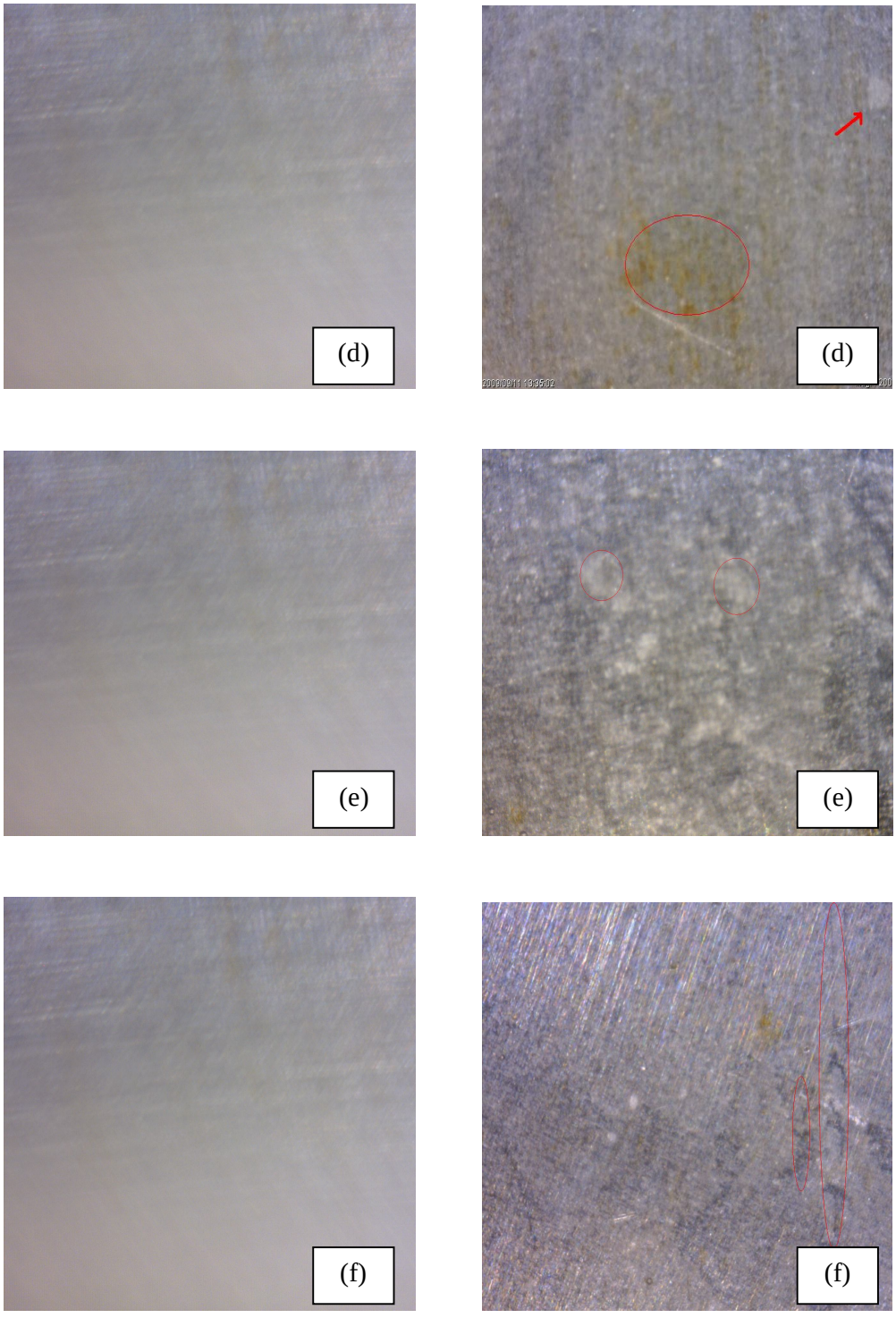

Fig. 4.29 Digital micrographs before (left) and after (right) 30days immersion in NaCl for sample (d) D, (e) E and (f) F.

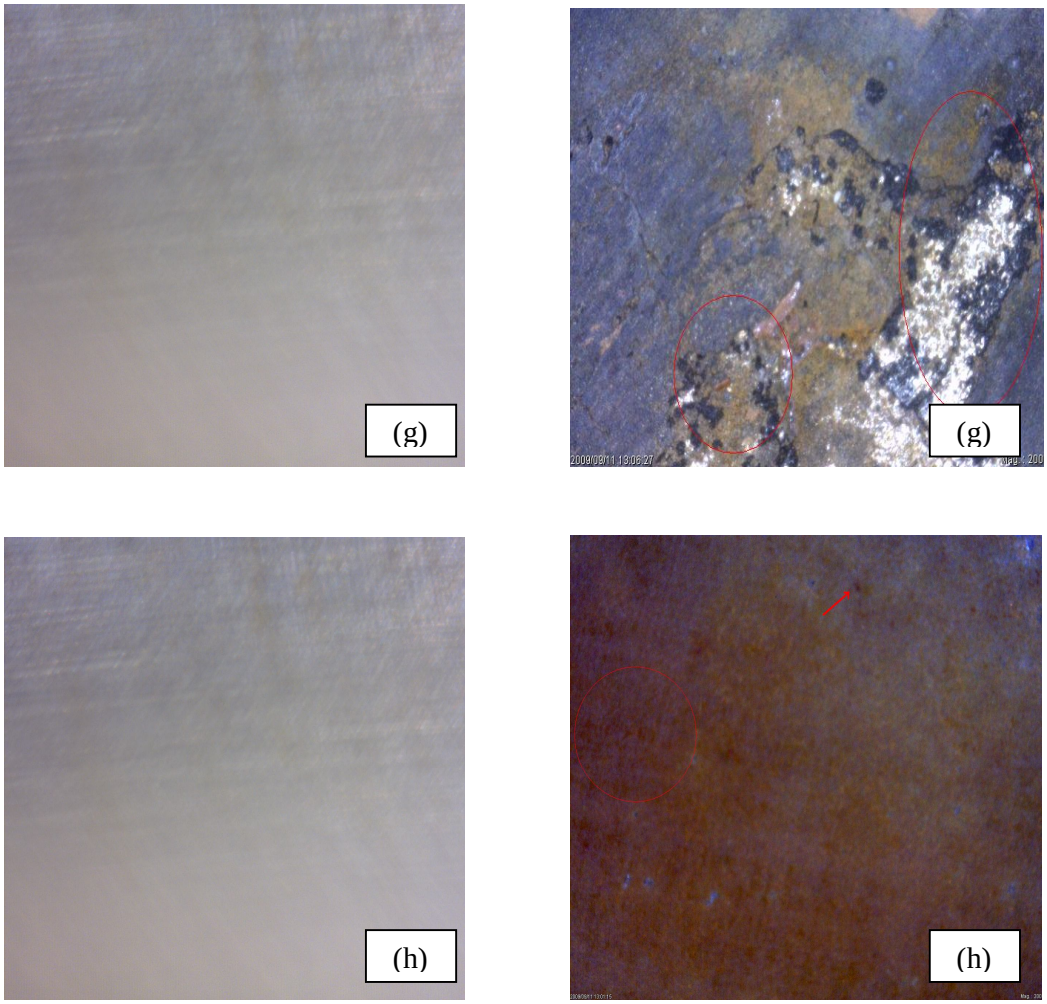

Fig. 4.30 Digital micrographs before (left) and after (right) 30days immersion in NaCl for sample (g) Blank 1 and (h) Blank 2

The digital micrographs for all samples before the immersion were almost similar. The entire surfaces were observed to be smooth with several fine polishing grooves. However, the micrographs differ after the immersion of samples in 3% NaCl. For samples cured at RT (A, B and C), the pitting phenomena were obvious. Moreover, the changes of the surface color of each sample were also observed. The changes of color were subjected to the rusting in which rusting proved that corrosion did occur to all the samples.

Sample A showed the least occurrence of pitting and its distribution was not uniform. Pitting distribution was greater and more uniform in sample B in which it

tends to accumulate at the edge of the sample. The most obvious pitting phenomena were observed in sample C in which it occurred almost at the entire surface of the sample. These results observed can be correlated to the corrosion rate values as discussed in section 4.6.

On the other hand, different conditions were to be observed for samples cured at 120° C. No pitting was determined in all samples. However, there were few blisters and a slight discoloration observed in all samples. Sample D (Figure 4.29d) shows a mild color changes and blisters. This is in agreement with the salt spray test result where the sampled produced the smallest amount of delamination hence only few blisters were observed on this sample. Sample E exhibits more blisters which were uniformly distributed at the surface of the sample. The same condition was detected at sample F but there were more blisters compared to sample E. In addition, there was a part of the surface where blisters looked like a "tunnel" in which this might create path for corrosion to occur. Usually, blistering occurs as a result of delamination and lost of adhesion. All these conditions observed are in agreement with the salt spray and adhesion test results which were discussed in previous sections.

Samples without PANI (Blank samples) show different micrographs than samples with PANI. For Blank 1 sample, it can be seen from Fig.4.30 (g) that the surface has been seriously damaged in which corrosion has taken place at almost the entire surface. Meanwhile, for Blank 2 sample, pitting was severe and the entire surface color has changed to brownish indicating the existence of rusts.

All the results obtained from the micrographs are in agreement with the salt spray, adhesion (pull-off) and impedance measurement (EIS) test. Basically, more pitting observed in samples cured at RT and Blank samples indicate that more severe corrosion occurred to the samples. Samples cured at 120° C (with PANI) exhibit the images of blisters and no pitting indicating that there were delamination of coating and decrease of adhesion with slight corrosion occurrence. All Blank samples exhibit micrographs with the worst surface conditions indicating that corrosion were significant for those samples. These results are supported with the drop of charge transfer resistance, R_{ct} noted earlier in the impedance measurement.

Samples particularly sample A, sample E and Blank 1 sample were also analyzed using the Scanning Electron Microscope (SEM). The results obtained from the SEM analysis show the same images with the images obtained from digital micrographs as shown in Figure 4.31. This indicates that digital micrograph is also reliable in providing the morphology of the samples.

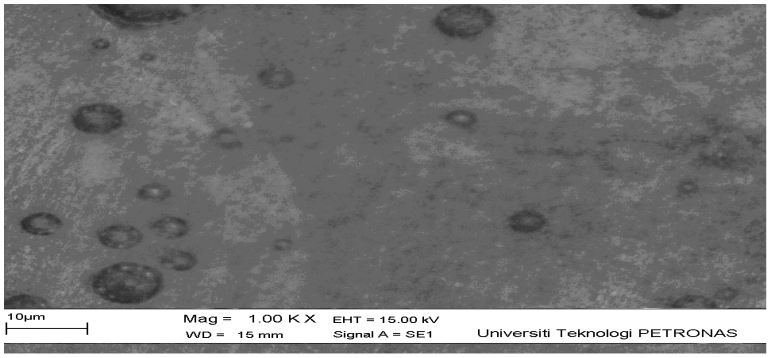

(a) Sample A

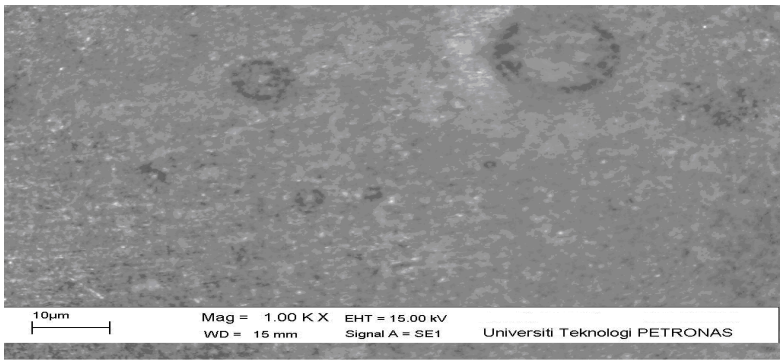

(b) Sample E

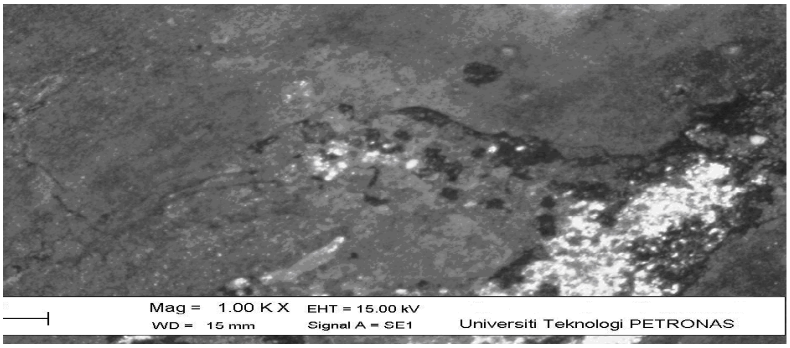

(c) Blank 1

Fig. 4.31 SEM micrographs after 30days immersion in NaCl for sample (a) Sample A, (b) Sample E and (c) Blank 1

4.8 Correlation of EIS with Other Corrosion Analysis

Results obtained from the impedance measurement need to be correlated with other corrosion analysis results such as salt spray test, pull-off test and water absorption test to determine whether or not they are compatible and similar to each other. In general, results obtained from EIS were consistent with results obtained from other corrosion tests.

4.8.1 EIS versus Salt Spray Test

The salt spray test revealed that there were formation of blisters and delamination occurred after 30 days of exposure to the salt spray chamber. By referring to Table 4.12, the values of double layer capacitance increased after 30 days of immersion in NaCl. This indicates that there were distributions of ions on unprotected metal surface. Unprotected metal surface are resulted from the delamination of the coatings. That is why the C_{dl} values and the delamination values were found to increase after 30 days of exposure to 3% NaCl. This is supported with the increase of corrosion rates of all samples as indicated in Table 4.13.

4.8.2 EIS versus Pull-off Test

For all samples, the wet adhesion measurements were determined to have decreased compared to the initial (dry adhesion). From the impedance measurement, there were decrease in the R_{ct} and increase in C_{dl} values after 30 days immersion. This is actually the consequence of the penetration of water or ions through the epoxy coating. The molecules of water / ions that reach the metal/epoxy coating interface compete for the adhesion sites and corrosion processes on a metal substrate are initiated. The bonds between metal and the epoxy coating are weakened because water has the tendency to accumulate at the interface, thereby replacing the bonds that exist between polymer and metal. As a result, the adhesion strengths of the epoxy coatings are reduced.

4.8.3 EIS versus Water Absorption

From the water absorption test, it shows that more water being absorbed with the increase of immersion time. This is in correlation with the capacitance values obtained from the impedance measurement. The increase of capacitance values can be interpreted as the consequence of continuous water being absorbed. The values of water being absorbed by the coatings increased when reaching the 30^{th} day of immersion simply because the barrier effect of PANI has decreased and this is proved by the increased of capacitance values.

4.8.4 EIS versus Morphological Analysis

The micrographs obtained from the morphological analysis correspond well with the corrosion rates obtained from the EIS measurement as shown in Table 4.13. As can be seen in Figure , samples cured at RT (A, B and C) exhibit corrosion (pitting) worse than samples cured at 120° C (D, E and F). Meanwhile, the worst corrosion conditions were determined to occur to the blank samples. This is in agreement with the corrosion rates obtained from the impedance measurement where the corrosion rates (CR) were found to increase in the following order: $CR_D < CR_E < CR_F < CR_A < CR_B < CR_C < CR_{Blank\ 1} < CR_{Blank2}$.